This is the peer-reviewed, final accepted version for American Mineralogist, published by the Mineralogical Society of America.
The published version is subject to change. Cite as Authors (Year) Title. American Mineralogist, in press.
DOI: https://doi.org/10.2138/am-2022-8539. http://www.minsocam.org/

21 September 2022 – REVISION #2 – Submitted to *American Mineralogist*

An evolutionary system of mineralogy, Part VII: The evolution of the igneous minerals (> 2500 Ma)

Robert M. Hazen[1,*] Shaunna M. Morrison[1],
Anirudh Prabhu[1], Michael J. Walter[1], and Jason R. Williams[1]
[1]Earth and Planets Laboratory, Carnegie Institution for Science,
5251 Broad Branch Road NW, Washington DC 20015, U. S. A.

Abstract

Part VII of the evolutionary system of mineralogy catalogs, analyzes, and visualizes relationships among 919 natural kinds of primary igneous minerals, corresponding to 1665 mineral species approved by the International Mineralogical Association – minerals that are associated with the wide range of igneous rock types through 4.566 billion years of Earth history. A systematic survey of the mineral modes of 1850 varied igneous rocks from around the world reveals that 115 of these mineral kinds are frequent major and/or accessory phases. Of these most common primary igneous minerals, 69 are silicates, 19 are oxides, 13 are carbonates, and 6 are sulfides. Collectively, these 115 minerals incorporate at least 33 different essential chemical elements.

Patterns of coexistence among these minerals, revealed by network, Louvain community detection, and agglomerative hierarchical clustering analyses, point to four major communities of igneous primary phases, corresponding in large part to different compositional regimes: (1) silica-saturated, quartz- and/or alkali feldspar-dominant rocks, including rare-element granite pegmatites; (2) mafic/ultramafic rock series with major calcic plagioclase and/or mafic minerals;

(3) silica-undersaturated rocks with major feldspathoids and/or analcime, including agpaitic rocks and their distinctive rare-element pegmatites; and (4) carbonatites and related carbonate-bearing rocks.

Igneous rocks display characteristics of an evolving chemical system, with significant increases in their minerals' diversity and chemical complexity over the first two billion years of Earth history. Earth's earliest igneous rocks (>4.56 Ga) were ultramafic in composition with 122 different minerals, followed closely by mafic rocks that were generated in large measure by decompression melting of those ultramafic lithologies (4.56 Ga). Quartz-normative granitic rocks and their extrusive equivalents (> 4.4 Ga), formed primarily by partial melting of wet basalt, added to the mineral inventory, which reached 246 different mineral kinds. Subsequently, four groups of igneous rocks with diagnostic concentrations of rare element minerals – layered igneous intrusions, complex granite pegmatites, alkaline igneous complexes, and carbonatites – all first appeared ~ 3 billion years ago. These more recent varied kinds of igneous rocks hold more than 700 different minerals, 500 of which are unique to these lithologies.

Network representations and heatmaps of primary igneous minerals illustrate Bowen's reaction series of igneous mineral evolution, as well as his concepts of mineral associations and antipathies. Furthermore, phase relationships and reaction series associated with the minerals of a dozen major elements (H, Na, K, Mg, Ca, Fe, Al, Si, Ti, C, O, and S), as well as minor elements (notably Li, Be, Sr, Ba, Mn, B, Cr, Y, REE, Ti, Zr, Nb, Ta, P, and F), are embedded in these multi-dimensional visualizations.

48 ***E-mail:** rhazen@carnegiescience.edu

49 ORCID 0000-0003-4163-8644

50

51 **Keywords:** philosophy of mineralogy; classification; mineral evolution; igneous petrology;

52 Bowen, Norman L.; phase equilibria; network analysis; carbonatites; alkaline igneous

53 complexes; Daly gap

54

This is the peer-reviewed, final accepted version for American Mineralogist, published by the Mineralogical Society of America.
The published version is subject to change. Cite as Authors (Year) Title. American Mineralogist, in press.
DOI: https://doi.org/10.2138/am-2022-8539. http://www.minsocam.org/

INTRODUCTION

A century ago, Canadian experimental petrologist Norman Levi Bowen (1887—1956) developed the concept of igneous rock evolution – the transformative idea that varied igneous rocks and their minerals display sequential "reaction series." In a brilliant portfolio of preliminary studies (e.g., Bowen 1912, 1913, 1915, 1922, 1927), subsequently integrated into his now-classic treatise *The Evolution of the Igneous Rocks* (Bowen 1928), Bowen synthesized and expanded on decades of field and experimental petrologic investigations to establish how a range of lithologies and their distinctive mineral inventories could emerge from a common parent magma (Yoder 1979, 1992, 1998).

Bowen's ideas have been instrumental in the ongoing development of an "Evolutionary System" of mineralogy (Hazen 2019). Like Bowen, we see ever more diverse suites of minerals arising from relatively simple and uniform starting conditions. Like Bowen, we recognize patterns of mineral diversity and complexity emerging as the result of deterministic, sequential, and congruent physical, chemical, and ultimately (in the case of minerals) biological processes. And, like Bowen, we employ the useful but restricted term "*evolution*" to denote a range of natural processes of chemical fractionation under varying conditions of temperature, pressure, and composition.

The resulting evolutionary system of mineralogy that we have devised is an attempt to chronicle the remarkable diversification of Earth's near-surface mineralogy through billions of years of planetary change. Parts I through V of the system (Hazen and Morrison 2020, 2021; Morrison and Hazen 2020, 2021; Hazen et al. 2021) catalogued minerals that record the earliest evolution of the solar system, as preserved in 294 meteorite phases. Part VI (Morrison et al.

2022) enumerated 262 of the earliest minerals that likely solidified following the Moon-forming impact (> 4.4 Ga), but prior to the oldest known terrestrial mineral (zircon that crystallized at ~4.4 Ga; Wilde et al. 2001; Valley et al. 2014). Collectively, the first six parts of the evolutionary system describe 442 natural kinds of minerals that represent Earth's earliest crustal inventory of solid phases (Morrison et al. 2022; their Supplementary Table 1). Note that we use the term "natural kind" in the sense of "categorizations that are conjectured to represent genuine divisions in nature in virtue of playing central roles in the articulation of successful scientific theories, … a grouping that is, in an important sense, independent of human conventions, interests, and actions" (Cleland et al. 2021; see also: Laporte 2004; Boyd 2010; Hawley and Bird 2011; Magnus 2012; Bird and Tobin 2015).

In Part VII, the midpoint of the evolutionary system of mineralogy, we chronicle 919 natural kinds of primary igneous minerals, corresponding to 1665 mineral species approved by the International Mineralogical Association's Committee on New Minerals, Nomenclature, and Classification (IMA-CNMNC; Burke 2006; Mills et al. 2009; Schertl et al. 2018). (Note that in this contribution we *italicize* the names of mineral natural kinds to distinguish them from IMA-CNMNC-approved mineral species.) These species represent a diverse, globally-distributed suite of minerals that have associations with a wide range of terrestrial igneous rock types. Investigation of relationships among these phases reveals a two-billion-year succession of physical and chemical processes that led inevitably from the earliest ultramafic and mafic rocks to evolving lithologies of increasing chemical and mineralogical complexity.

Igneous rocks, through chemical and physical actions of fractionation, differentiation, and partial melting, exemplify the sequential processing of crust and mantle materials on Earth and

other worlds and thus have been central to the development of the concept of mineral evolution. Although no terrestrial rocks are known to have been preserved from the earliest Hadean Eon, Morrison et al. (2022) suggest that Earth's first igneous rocks displayed a limited range of compositions and associated mineralogies, as manifest in the 67 primary igneous phases described in Part VI of this series. This limited suite of minerals from ultramafic and mafic lithologies was proposed on the basis of: (1) the primary asteroidal phases found in the mafic and ultramafic lithologies of stony achondrite meteorites, which represent fragments of crusts and mantles from the earliest differentiated planetessimals of the solar system, combined with (2) petrologic models of the crystallization and differentiation of Earth's post-lunar crust and mantle, primarily from cooling of a global magma ocean (Rollinson 2007; Van Kranendonk et al. 2007; Moynier et al. 2010; Badro and Walter 2015; Trønnes et al. 2019; Korenaga 2021).

However, over the following 2 billion years igneous lithologies evolved dramatically, with a concomitant increase in mineral diversity. By the end of the Archean Eon (2.5 Ga), primary igneous rocks spanned a wide range of chemical environments, underscoring the importance of gradual element differentiation and concentration in generating exotic suites of minerals.

In this study, we enumerate 919 natural kinds of primary igneous minerals and place those minerals in their sequential evolutionary contexts (Appendix I). This work highlights distinctive patterns of mineral co-occurrence, while exploring phase relationships preserved in the equilibrium mineral assemblages of igneous rocks. In particular, extensive tabulations of mineral co-existence data provide an ideal application of mineral network analysis (Newman 2010; Morrison et al. 2017), community structure analysis (Girvan and Newman 2002;

Fortunato 2010), and hierarchical cluster analysis (Maimon and Rokach 2006; Galli et al. 2018).

This work is presented in four main sections. Section I briefly describes the assembly of a data resource that records the coexisting primary minerals in 1850 diverse igneous rocks. The second part applies network analysis, community detection, and hierarchical clustering to explore patterns of mineral coexistence in igneous rocks. Section III explores several implications of these data-driven approaches for discovery and prediction in the field of igneous petrology. Finally, Appendix I details the nature and distribution of 115 of the most common primary minerals in those rocks, as well as the modified nomenclature employed in this contribution for some mineral kinds.

This is the peer-reviewed, final accepted version for American Mineralogist, published by the Mineralogical Society of America.
The published version is subject to change. Cite as Authors (Year) Title. American Mineralogist, in press.
DOI: https://doi.org/10.2138/am-2022-8539. http://www.minsocam.org/

I. ON THE DISTRIBUTION OF PRIMARY MINERALS IN IGNEOUS ROCKS

An examination of the modes of formation of all mineral species approved by the IMA-CNMNC (https://rruff.info/ima, accessed 20 January 2022) reveals 1665 mineral species that have been reported as primary igneous phases [Supplementary Table 1 and associated Supplementary Read-Me File 1; see also Hazen and Morrison (2022; their Supplementary Table 1 and additions)]. Note that Table 1 catalogs the six Supplementary Tables and three interactive graphical figures associated with this contribution. We have consolidated and modified the list of 1665 IMA-approved minerals to recognize 919 "natural kinds" (Hawley and Bird 2011; Magnus 2012; Bird and Tobin 2015; Hazen 2019; Cleland et al. 2021) of primary igneous minerals [Appendix I; Supplementary Table 2 and associated Supplementary Read-Me File 2; see also Hazen et al. 2022, their Supplementary Table 1 and additions)]. Supplementary Table 2 lists the distribution of these phases among the following 8 major groups of igneous rocks, each with distinctive mineral assemblages and each designated by the 3-letter abbreviation emplyed by Hazen and Morrison (2022).

1. Ultramafic rocks (UMA) are dominated by select mafic minerals, most frequently forsterite and/or Mg-rich clinopyroxene, and with < 5 vol % calcic plagioclase. Morrison et al. (2022) have proposed that these rocks were the earliest to appear at or near Earth's surface and thus have been almost continuously present since the planet's formation at ~4.566 Ga.
2. Mafic rocks (MAF), typically incorporate >> 5 vol % calcic plagioclase, one or more major mafic minerals, and < 5 vol % quartz; but also include rocks with > 40 vol % mafic minerals, >5 vol % alkali feldspar, and < 5 vol % quartz [e.g., Johannsen's (1937)

meta-kalisyenites]; and anorthosites and other rocks with with > 50 vol % calcic plagioclase. Mafic rocks are predominant among achondrite meteorites and we suggest that they were also among the earliest lithologies at Earth's surface, forming prior to 4.56 Ga (Morrison et al. 2022).

3. Granitic quartzo-feldpathic intrusive rocks (GRA) typically contain >> 5 vol % quartz and alkali feldspar; but also include alkali syenites with Na/K feldspar >> 50 vol %. Granitic lithologies were initially derived by partial melting of hydrated basalt, with subsequent formation through melting of Si-rich sediments (e.g., Yoder 1979; Philpotts and Ague 2009). Granite formation, which played a major role in the origin and growth of continents, is thought to have begun prior to 4.4 Ga (e.g., Wilde et al. 2001).
4. Rhyolitic silica-rich extrusive rocks (RHY) are characterized by rapidly-cooled phases, including tridymite, sanidine, and/or obsidian. These lithogies are genetically related to intrusive quartzo-feldspathic rocks and formed during the same time interval. We distinguish them because of their distinctive high-temperature/low-pressure phases and Si-rich glass component.
5. Rare-element "complex" granite pegmatites (CGP) are characterized by significant enrichments in Li, Be, B, and other incompatible elements relative to average crustal abundances, leading to distinctive minerals such as beryl, lepidolite, spodumene, and tourmaline. No known examples are older than 3 billion years (London 2008), which suggests that more than a billion years of element selection and concentration in the crust and upper mantle were required to produce minerals enriched in these

This is the peer-reviewed, final accepted version for American Mineralogist, published by the Mineralogical Society of America.
The published version is subject to change. Cite as Authors (Year) Title. American Mineralogist, in press.
DOI: https://doi.org/10.2138/am-2022-8539. http://www.minsocam.org/

175 elements. The concentration of incompatable elements was most likely enhanced by
176 subduction-related processes (Bradley 2011; Tkachev 2011; Grew and Hazen 2014;
177 Hazen et al. 2014; Nance et al. 2014).

178 6. Silica-undersaturated alkaline (miaskitic and agpaitic) rocks (AGP) incorporate > 5 vol
179 % feldspathoid minerals and/or analcime. They include rare-element agpaitic
180 pegmatites with minerals incorporating rare-earth elements (REEs), Zr, Nb, Ta, and
181 other incompatible elements (Mitchell 1996a, 1996b; Marks and Markl 2017). These
182 distinctive alkaline lithologies require significant melt evolution; consequently, the
183 oldest known examples are < 3 Ga.

184 7. Carbonatites and related carbonate-rich rocks (CAR) feature one or more carbonate
185 minerals as a major phase. Carbonatites are a common and widespread igneous
186 lithology throughout the past 3.0 Ga, despite being a volumetrically minor
187 component of the crust and upper mantle (Woolley 1987, 2001, 2019; Kogarko et al.
188 1995; Bizzarro et al. 2002; Wooley and Kjarsgaard 2008; Jones et al. 2013;
189 Kamenetsky et al 2021). Of special note are a suite of rare element accessory
190 minerals (Chakhmouradian 2006; Christy et al. 2021) that often result in economically
191 valuable concentrations of REE and other resources (Simandl and Paradis 2018;
192 Anenburg et al. 2021).

193 8. Layered igneous intrusions (LAY) incorporate the same major minerals as
194 ultramafic/mafic/intermediate igneous rock series but are distinguished by their
195 diagnostic mineralogy, including significant concentrations of rare minerals
196 containing platinum group elements (PGEs), as well as concentrations of chromite,

This is the peer-reviewed, final accepted version for American Mineralogist, published by the Mineralogical Society of America.
The published version is subject to change. Cite as Authors (Year) Title. American Mineralogist, in press.
DOI: https://doi.org/10.2138/am-2022-8539. http://www.minsocam.org/

magnetite, and ilmenite (Maier 2005; Mungall and Naldrett 2008). The oldest known PGE-enriched layered igneous intrusions are ~2.7 to 2.8 Ga, and thus significantly postdate the ultramafic and mafic rocks that are thought to have dominated crustal igneous rocks in the early Hadean Eon (Rollinson 2007; Van Kranendonk et al. 2007; Moynier et al. 2010; Badro and Walter 2015; O'Driscoll and Van Tongeren 2017; Trønnes et al. 2019; Korenaga 2021).

We acknowledge that there exist significant overlaps—compositionally, mineralogically, and temporally—among some of these 8 broad categories of igneous rocks. Nevertheless, each group displays its own characteristic suite of minerals (e.g., Deer et al. 1982-2013; Anthony et al. 1990-2003), and each has a distinctive history in the evolutionary system.

Mineral modes of igneous rocks: The core data of this study are found in Supplementary Table 3 (see also Supplementary Read-Me File 3), which details the distribution of 115 of the most common primary igneous minerals among 1850 igneous rock modes. In constructing this data resource, we relied heavily on the monumental *Descriptive Petrography of the Igneous Rocks* of Albert Johannsen (1932, 1937, 1938), who documented mineral modes for more than 1000 varied igneous rocks. We added 795 igneous rock modes from a wide range of alkaline rocks and carbonatites (Woolley 1987, 2001, 2019; Kogarko et al. 1995), as well as modal data on other igneous rocks (Deer et al. 1982-2013; https://mindat.org, accessed 20 January 2022; see Appendix I).

This is the peer-reviewed, final accepted version for American Mineralogist, published by the Mineralogical Society of America.
The published version is subject to change. Cite as Authors (Year) Title. American Mineralogist, in press.
DOI: https://doi.org/10.2138/am-2022-8539. http://www.minsocam.org/

II. MINERAL ASSOCIATIONS AND ANTIPATHIES:

DATA ANALYSIS AND VISUALIZATION OF PRIMARY IGNEOUS MINERALS

"The evidences of fractional crystallization or crystallization-differentiation in magmas … consist in the mineral associations and antipathies which they characteristically display."

N. L. Bowen, *The Evolution of the Igneous Rocks* (1928, p.20)

Bowen (1928) employed patterns of "mineral associations and antipathies" in the development of his theory of igneous rock evolution. He recognized that some pairs of minerals are frequently encountered: "Rocks rich in quartz tend to be rich in orthoclase or sodic plagioclase or both. If a rock has hornblende as its most important ferromagnesian constituent it is likely to have intermediate plagioclase as its principal feldspathic component. If the feldspathic mineral is basic plagioclase, pyroxene with or without olivine tends to be the principal femic constituent" (Bowen 1928, p. 21).

On the other hand, many pairs of minerals – *quartz/forsterite* or *quartz/nepheline*, for example – never coexist in equilibrium, because phases of intermediate compositions occur. Bowen called these examples of mineral antipathies "actual incompatibilities … which have a purely chemical basis." He also recognized "incompatibilities of a different kind, based wholly on petrogenetic factors," such as the rarity of the mineral pairs *quartz/anorthite*, *orthoclase/forsterite*, or *quartz/augite* – such combinations are "too far apart in a crystallization sequence to make up the entire rock."

In this section we amplify Bowen's approach by quantifying the extent of coexistence among pairs and larger groupings of 115 common primary minerals of igneous rocks, including a wide range of major and accessory (notably rare-element) minerals. Employing data on the primary

This is the peer-reviewed, final accepted version for American Mineralogist, published by the Mineralogical Society of America.
The published version is subject to change. Cite as Authors (Year) Title. American Mineralogist, in press.
DOI: https://doi.org/10.2138/am-2022-8539. http://www.minsocam.org/

minerals in 1850 igneous rock modes (Supplementary Table 3), we tabulate the frequency of co-occurrence of every pairwise combination of these 115 mineral kinds (Supplementary Table 4; see also associated Supplementary Read-Me File 4). Then, for each mineral pair we calculate the percentage of the less common mineral that co-occurs with the more common mineral (Supplementary Table 5; see also Supplementary Read-Me File 5). For example, we record 487 rocks that contain *hornblende* and 330 rocks that contain *ilmenite*, of which 89 rocks contain both minerals (Supplementary Table 4, matrix elements Y25, Z26, and Z25, respectively). Therefore, 27 % of occurrences of the less frequent mineral (*ilmenite*) also occur with *hornblende* (Supplementary Table 5, matrix element Z25).

This approach is especially important in the case of a relatively rare accessory mineral coexisting with an abundant major phase: For example, we record only 22 rocks that incorporate the Ca-REE-carbonate *parisite* in our tabulations; however, *parisite* co-occurs with the commonest igneous mineral *fluorapatite* (1234 occurences) in 14 (64 %) of those rocks. Thus, *fluorapatite*/*parisite* is a likely mineral pair whenever the rare mineral *parisite* occurs. As Bowen emphasized, we find that some mineral pairs usually occur together (*arfvedsonite/eudialyte*, *beryl/elbaite*, *fluorapatite/phlogopite*), whereas many other mineral pairs are rarely or never observed (*forsterite/microcline*, *albite/monticellite*, *nepheline/quartz*). Analysis of this broader range of mineral associations and antipathies – especially consideration of rare-element accessory phases – points to sequences of mineral formation that may expand on Bowen's concept of "reaction series," for example by documenting the crystallization behavior of minor phases with rare elements. We employ three types of data visualization: unipartite networks that highlight Louvain community detection, heat maps showcasing

agglomerative hierarchical clustering, and bipartite networks representing relationships among minerals and their formational environments.

Unipartite networks and Louvain community detection analysis of coexisting igneous minerals: Network analysis, perhaps best known for characterizing relationships within human social networks (e.g., Newman 2010), provides powerful tools for identifying patterns among coexisting minerals (Morrison et al. 2017). Accordingly, Figures 1A and 1B display unipartite networks that illustrate the coexistence of the 115 most common igneous minerals, as listed in Table 2. These graphs were built on "Observable" (https://observablehq.com/), using D3js (Bostock et al. 2011). The networks use the D3-force algorithm (https://d3-wiki.readthedocs.io/zh_CN/master/Force-Layout/) for its network layout. The code and an interactive version of this network can be found at: https://observablehq.com/@anirudhprabhu/evol_sys_part7_unipartite (for instructions, see Figure 1 caption).

Each of the 115 nodes in Figure 1 represents a mineral kind, with the size of the node and lettering in Figure 1A indicating the relative abundance of that mineral in our tabulations of 1850 igneous rock modes (Supplementary Table 3). Links between pairs of nodes indicate mineral coexistence. in Figure 1A, we illustrate the case where at least 49 % of occurrences of the less common mineral coexist with the more common mineral (based on percentages tabulated in Supplementary Table 5). Figure 1 is a static rendering of a dynamic interactive network in which the co-occurrence percentage, *P*, can be varied continuously from 1 to 100 %.

This is the peer-reviewed, final accepted version for American Mineralogist, published by the Mineralogical Society of America.
The published version is subject to change. Cite as Authors (Year) Title. American Mineralogist, in press.
DOI: https://doi.org/10.2138/am-2022-8539. http://www.minsocam.org/

This variable feature, as well as other interactive aspects of the online version of Figure 1, facilitates studies of mineral associations and antipathies, as highlighted by Bowen (1928).

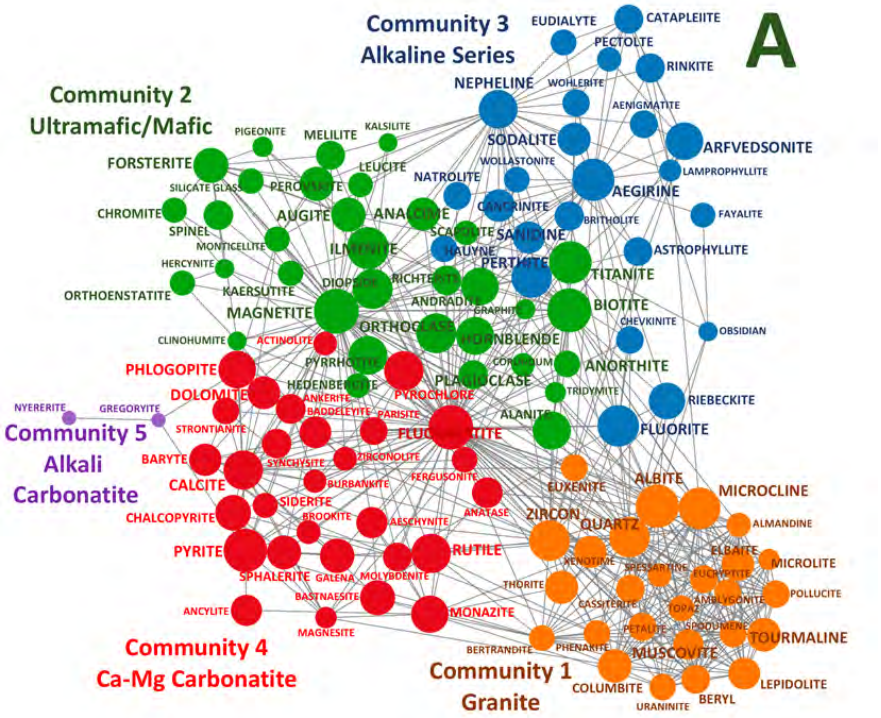

This is the peer-reviewed, final accepted version for American Mineralogist, published by the Mineralogical Society of America.
The published version is subject to change. Cite as Authors (Year) Title. American Mineralogist, in press.
DOI: https://doi.org/10.2138/am-2022-8539. http://www.minsocam.org/

Figure 1. **(A)** A unipartite network of 115 common primary igneous minerals (colored circles), with links between pairs of coexisting minerals. Node and lettering sizes indicate the relative abundances of minerals, while colors indicate four large communities of igneous minerals that were determined using Louvain community detection (see text). Each of these four communities corresponds to the mineralogy of a major rock group. *Community 1*: Orange nodes represent 26 minerals from granitic rocks with dominant quartz and/or alkali feldspar. *Community 2*: 34 green nodes represent minerals from primarily mafic and ultramafic rocks with dominant calcic plagioclase and/or mafic minerals. *Community 3*: Blue nodes represent 24 minerals in alkaline rocks with dominant felspathoids. *Community 4*: 29 red nodes correspond to minerals in carbonatites with major Ca-Mg carbonate minerals. *Community 5*: Two purple nodes represent alkali carbonatites, as exemplified by the Oldoinyo Lengai carbonatite volcano in Tanzania. **(B)** The unipartite network of 115 primary igneous minerals embeds every igneous rock type as a sub-graph. Highlighted examples include muscovite granite, olivine gabbro, nepheline syenite, and calcite carbonatite. In this figure, links are drawn between two minerals if at least 49 % of rocks that incorporate the less common mineral also incorporate the more common mineral (as tabulated in Supplementary Table 3). One can vary this percentage in an interactive version of this graph at: [https://observablehq.com/@anirudhprabhu/evol_sys_part7_unipartite]. Hover your cursor over any node to identify the corresponding mineral; click and hold your cursor to move that node and identify links to other nodes; use your cursor to move the "Weight Threshold" vernier to systematically eliminate links between nodes based on *P* values (see text).

Links in networks are not typically uniformly distributed. For example, in Figure 1 nodes form communities that reflect strongly interconnected groups of minerals within the larger structure. In this contribution, we have applied two different methods to identify these groups of primary igneous minerals – Louvain community detection and agglomerative hierarchical clustering. The

mineral nodes in Figure 1A are colored based on Louvain community detection analysis (Girvan and Newman 2002; Fortunato 2010), which is a method to extract the community structure of large networks that employs a heuristic method based on modularity optimization (Blondel et al. 2008). This community detection method identifies members of a group iteratively in two phases: (1) small communities (starting with each node being its own distinct community) are formed at a local level by maximizing modularity of certain nodes; (2) each small community is aggregated into one "super node" to form a new "super node network" and the first step is repeated until there are no changes in the network and the modularity has been optimized. The Louvain modularity approach does not require a user to specify the number of clusters in a dataset, which removes some of the bias associated with many other clustering algorithms. Consequently, this analytical approach identifies the most closely interconnected subsets of minerals We observe four principal communities of igneous primary phases, corresponding to four major groups of igneous rocks (Figure 1B), which are also listed in Table 2:

Community 1: Twenty-six compactly-grouped minerals (colored orange in Figure 1A) represent quartz- and/or alkali feldspar-dominant rocks, including rare-element granite pegmatites. An important feature of these minerals is a suite of diagnostic accessory phases incorporating Li (*eucryptite*; *lepidolite*; *petalite*; *spodumene*), Be (*bertrandite*; *beryl*; *euclase*; *phenakite*), B (*elbaite*; *tourmaline*), Cs (*pollucite*), Ta/Nb (*columbite*; *euxenite*; *microlite*), Sn (*cassiterite*), Th (*thorite*), and U (*uraninite*).

Community 2: Ultramafic and mafic rocks relatively poor in silica, many with major calcic plagioclase and/or mafic minerals but also silica-undersaturated rocks with analcime, kalsilite, leucite, and/or scapolite, are represented by 34 green nodes in Community 2

This is the peer-reviewed, final accepted version for American Mineralogist, published by the Mineralogical Society of America.
The published version is subject to change. Cite as Authors (Year) Title. American Mineralogist, in press.
DOI: https://doi.org/10.2138/am-2022-8539. http://www.minsocam.org/

– the largest of the 5 communities in Figure 1A. This suite contains several of the most common primary igneous minerals, including *biotite*, *ilmenite*, *magnetite*, and *titanite*, all of which are present in a wide range of lithologies and thus play prominent central roles in the network. By contrast, Community 2 includes only one rare-element accessory mineral – the rare earth element (REE) Ca-silicate *allanite*, which is the most frequently encountered REE igneous mineral. This lack of rare element phases in Community 2 mirrors the relatively low concentrations of incompatible elements in mafic and ultramafic rocks compared to other lithologies. Community 2 displays a number of strong connections among other communities. For example, *allanite* is close to the REE minerals *euxenite* and *xenotime* in Community 1. Similarly, the Community 2 sulfide *pyrrhotite* is close to Community 4 with several other sulfide minerals. And the sub-silicic phases *analcime*, *kalsilite*, *leucite*, and *scapolite* all border Community 3, which includes *nepheline*, *sodalite*, *cancrinite* and other phases most commonly associated with undersaturated alkaline igneous rocks.

Community 3: Community 3 encompasses 24 minerals (blue nodes) in igneous rocks from silica-undersaturated alkaline rocks with major *nepheline*, *sodalite*, and/or *cancrinite*, including agpaitic rocks and their distinctive rare-element pegmatites. These lithologies are notable for diagnostic accessory minerals that concentrate high-field-strength elements (HFSE), including Y/REE (*britholite*; *chevkinite*; *rinkite*), Ti (*aenigmatite*; *astrophyllite*; *lamprophyllite*; *wohlerite*), and Zr (*catapleite*; *eudialyte*).

Community 4: Twenty-nine minerals, shown as red nodes in Figure 1A, occur in carbonatites and related rocks with major calcite, dolomite, and/or Fe-bearing

This is the peer-reviewed, final accepted version for American Mineralogist, published by the Mineralogical Society of America.
The published version is subject to change. Cite as Authors (Year) Title. American Mineralogist, in press.
DOI: https://doi.org/10.2138/am-2022-8539. http://www.minsocam.org/

carbonate minerals. This mineralogically distinct community features 11 of 13 primary igneous carbonates in our list of 115 of the most common primary igneous phases, as well as 5 of 6 sulfides, the only sulfate (*baryte*), 2 of 4 phosphates, and 8 of 20 oxides. By contrast, Community 4 includes only 2 of 69 silicates (*actinolite* and *phlogopite*). Carbonatites are notable for numerous rare-element accessory phases, including Y/REE oxides (*aeschynite*; *fergusonite*; *zirconolite*), carbonates (*ancylite*; *bastnaesite*; *burbankite*; *parasite*; *synchesite*), and the phosphate *monazite*. Also of note are common accessory minerals of Sr and Ba (*ancylite*; *baryte*; *burbankite*; *strontianite*; *syneschite*), which, with the exception of the Sr-Ba silicate *lamprophyllite* in Cluster 3, are not observed in the other groups. Rare-element, HFSE accessory minerals in Community 4 also incorporate Nb/Ta (*aeschynite*; *fergusonite*; *pyrochlore*); Ti (*aeschynite*; *anatase*; *brookite*; *rutile*), and Zr (*baddeleyite*; *zirconolite*).

Community 5: Two rare alkali carbonatite minerals, *fergusonite* and *gregoryite*, are represented by purple nodes in Figure 1A and constitute their own Community 5 in our analysis. The principal locality for these minerals is Oldoinyo Lengai in Tanzania, which is the world's only active carbonatite volcano. Alkali carbonates are ephemeral compared to those of Ca-Mg-Fe carbonatites; therefore, it is not certain whether they have represented a significantly greater proportion of carbonatites in the past (Zaitsev and Keller 2006).

We performed similar Louvain community detection analysis for different values of percentage of co-occurrence: P = 1, 49, and 75 %. With the exception of mineral nodes that

This is the peer-reviewed, final accepted version for American Mineralogist, published by the Mineralogical Society of America.
The published version is subject to change. Cite as Authors (Year) Title. American Mineralogist, in press.
DOI: https://doi.org/10.2138/am-2022-8539. http://www.minsocam.org/

were no longer connected to the network at P = 75 %, the four main communities appear to be independent of *P*.

Of special interest is the degree of connectivity, or network density, of the graph in Figure 1, which varies signficantly with the percentage of co-occurrence, *P*. The density of a network (*D*) is defined as the fraction of all possible links that are observed; in the case of 115 minerals, there exist $[(115^2 – 115)/2] = 6555$ possible links. When *P* = 1 %, the density of the network has a relatively high value of *D* = 0.51, because 3359 (51 %) of the 6555 possible links between mineral pairs are observed to occur at least once. By contrast, when we restrict links to *P* = 25 % then only 1426 links remain (*D* = 0.22). And when we consider *P* = 49 % (the highest percentage for which all 115 minerals are still linked to at least one other mineral), only 608 links persist – a relatively sparse network with *D* = 0.093.

Note that at *P* > 49 %, one or more mineral nodes is no longer connected to the network. The first nodes to disconnect are *obsidian*, *kalsilite*, and the two alkali carbonates *gregoryite* and *nyererite*, all of which disconnect at *P* = 50 %. At *P* = 75 %, only 74 of the original 115 mineral nodes remain interconnected in a sparse, dispersed network (*D* = 0.063) with only 170 links out of a possible 2701.

An important feature of the unipartite networks of primary igneous minerals is that every igneous rock, for example each of the 1850 examples in Supplementary Table 3, is represented as a multi-node subgraph of this network (Figure 1B; see also Morrison et al. 2017, their Figure 1B). Thus, Figure 1 and related networks are useful visual approaches to comparing and contrasting aspects of igneous petrology for research and education.

This is the peer-reviewed, final accepted version for American Mineralogist, published by the Mineralogical Society of America.
The published version is subject to change. Cite as Authors (Year) Title. American Mineralogist, in press.
DOI: https://doi.org/10.2138/am-2022-8539. http://www.minsocam.org/

Agglomerative hierarchical cluster analysis and heatmap visualization of coexisting igneous minerals: Patterns of co-occurrence among the 115 primary igneous minerals were visualized as a heatmap using the *heatmaply* package of R (Galili et al. 2018), with the sequence of minerals determined by agglomerative hierarchical clustering (Maimon and Rokach 2006). Note that both methods employed in this study are agglomerative (or "bottom up") approaches that commence with pairwise mineral groupings and add minerals to form larger communities or clusters until all minerals are combined into a single cluster.

We supplied a 115 x 115 data matrix representing the percentages of co-occurrences between pairs of igneous minerals (Supplementary Table 5) to the *heatmaply* function. This function performed an agglomerative hierarchical clustering algorithm with a complete linkage approach to map minerals in the heatmap, so that those phases with higher percentages of co-occurrences were placed closer to one another. Each matrix element represents the co-occurrence of two minerals; each is colored, with brighter colors indicating higher percentages of co-occurrence. Figure 2 thus provides an alternative approach to visualizing mineral associations and antipathies – one that is complementary to the Louvain community detection algorithm applied to the primary mineral coexistence data in Figure 1A. Note that Figure 2 is a static view of an interactive graphic (see Figure 2 caption), which can be accessed at: https://dtdi.carnegiescience.edu/sites/all/themes/bootstrap-d7-theme/networks/HeatmapIgnPercentColorize.html.

An important feature of hierarchical cluster analysis is that one can examine the "tree diagrams" on the top (and, equivalently, on the righthand side) of Figure 2 to select any desired number of clusters, from merging all minerals into a single cluster, to 115 clusters, each of which is a different mineral. In order to compare this approach to the unipartite network of

This is the peer-reviewed, final accepted version for American Mineralogist, published by the Mineralogical Society of America.
The published version is subject to change. Cite as Authors (Year) Title. American Mineralogist, in press.
DOI: https://doi.org/10.2138/am-2022-8539. http://www.minsocam.org/

Figure 1A, we identified and examined four major clusters of minerals arranged along the diagonal axis and designated Clusters A through D (i.e., Figures 3A through 3D), with two additional clusters, each containing only two minerals (Clusters E and F). The minerals in each cluster (denoted A through F), and their correspondence to Communities 1 through 5 in Figure 1A, are identified in Table 2.

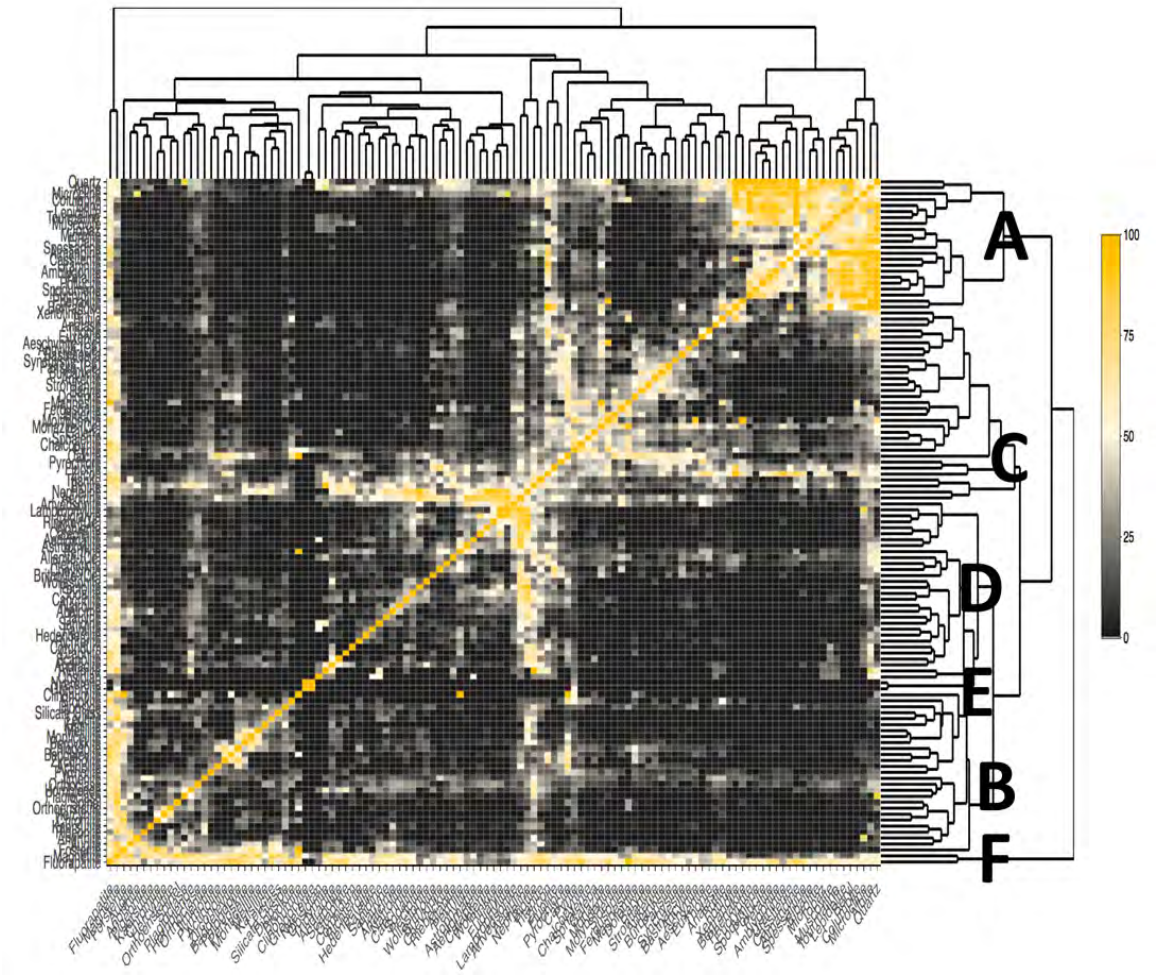

Figure 2. This "heat map" is a 115 x 115 diagonally symmetrical matrix of coexisting primary igneous minerals, with 6555 unique non-diagonal matrix elements. Each matrix element represents the percentage of the rarer mineral that coexists with the more common mineral (Supplementary Table 5; see text), as defined by the color scale. Minerals that occur frequently together are indicated by more brightly colored matrix elements. The order of minerals from top to bottom (and, equivalently, from right to left) was determined by agglomerative hierachical cluster analysis using the *heatmaply* package

This is the peer-reviewed, final accepted version for American Mineralogist, published by the Mineralogical Society of America.
The published version is subject to change. Cite as Authors (Year) Title. American Mineralogist, in press.
DOI: https://doi.org/10.2138/am-2022-8539. http://www.minsocam.org/

436 of R (Galili et al. 2018), which grouped minerals according to their associations. Adjacent pairs of
437 minerals are most closely related, with larger groups arranged hierarchically, as indicated by the
438 hierachical tree on the top (and, equivalently, the righthand side) of the matrix. We consider 6 clusters,
439 labeled A to F (see text). See Figures 3A to 3E for enlargements of specific areas. For an interactive
440 version of this figure, go to: https://dtdi.carnegiescience.edu/sites/all/themes/bootstrap-d7-
441 theme/networks/HeatmapIgnPercentColorize.html. Open this link and move your cursor over any matrix element
442 to see the corresponding pair of minerals and their percentage of co-occurrence.
443

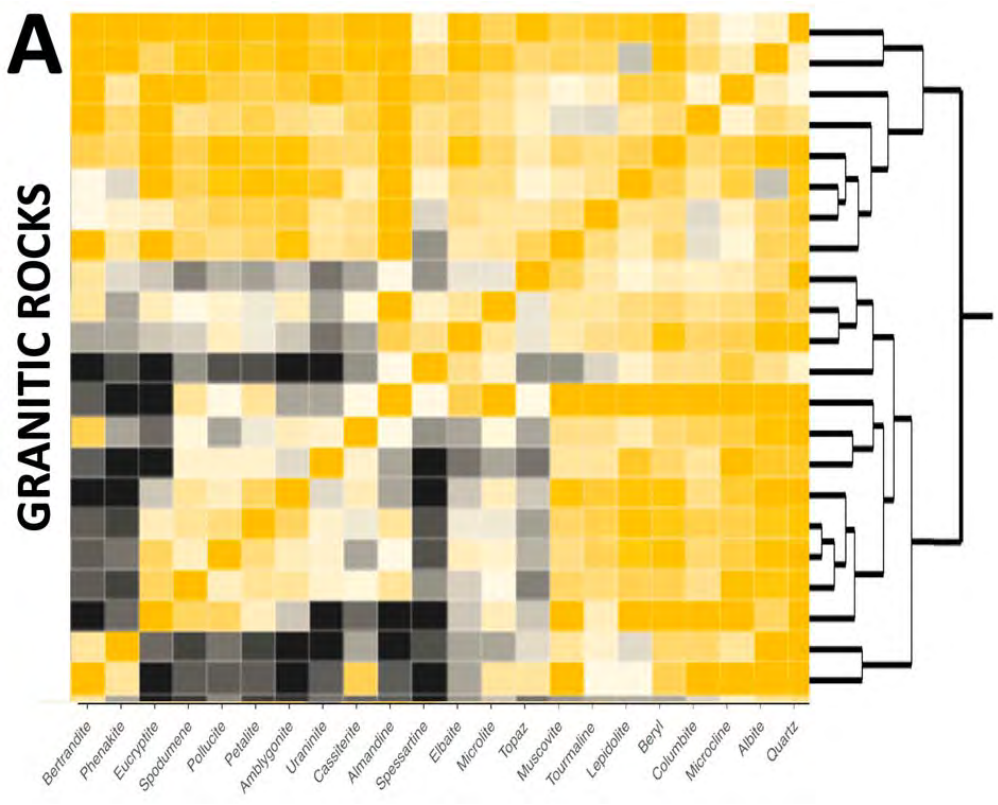

444

This is the peer-reviewed, final accepted version for American Mineralogist, published by the Mineralogical Society of America.
The published version is subject to change. Cite as Authors (Year) Title. American Mineralogist, in press.
DOI: https://doi.org/10.2138/am-2022-8539. http://www.minsocam.org/

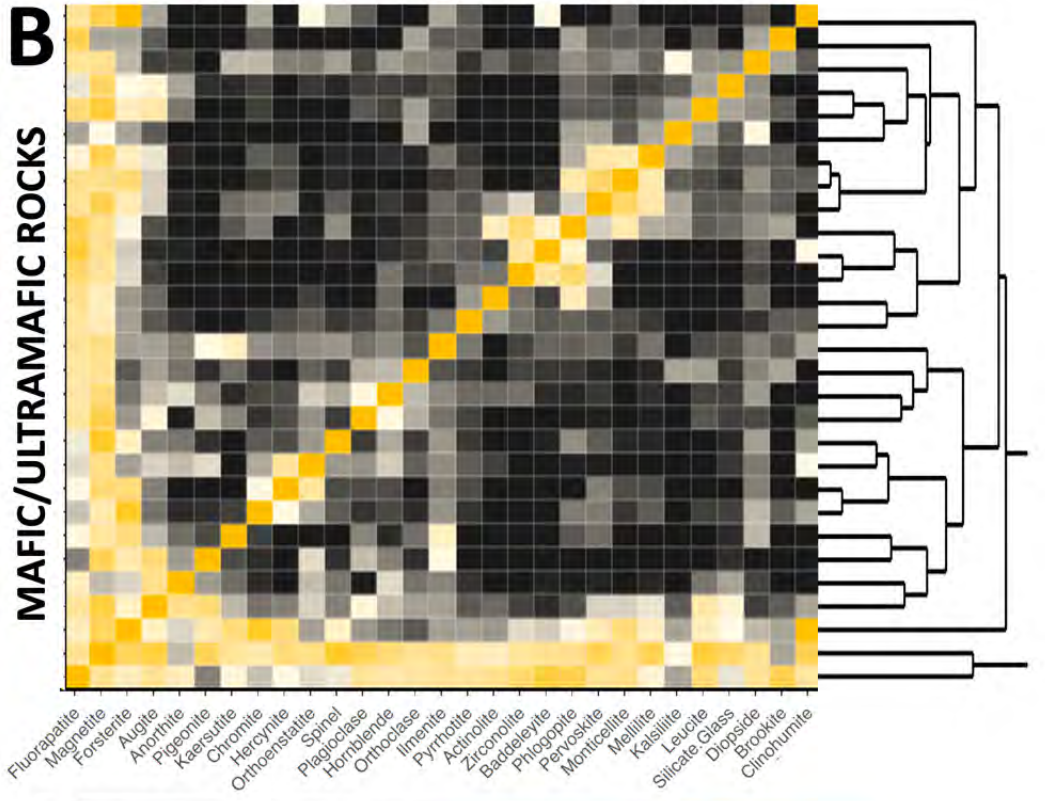

445

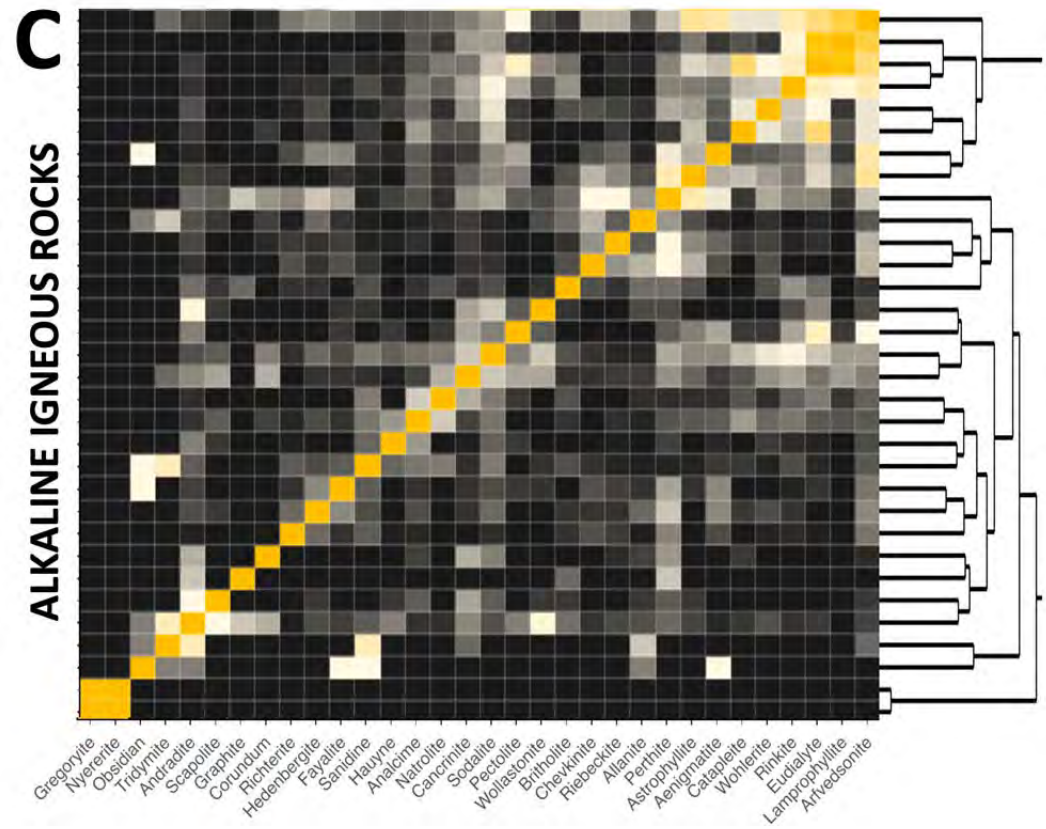

446

This is the peer-reviewed, final accepted version for American Mineralogist, published by the Mineralogical Society of America.
The published version is subject to change. Cite as Authors (Year) Title. American Mineralogist, in press.
DOI: https://doi.org/10.2138/am-2022-8539. http://www.minsocam.org/

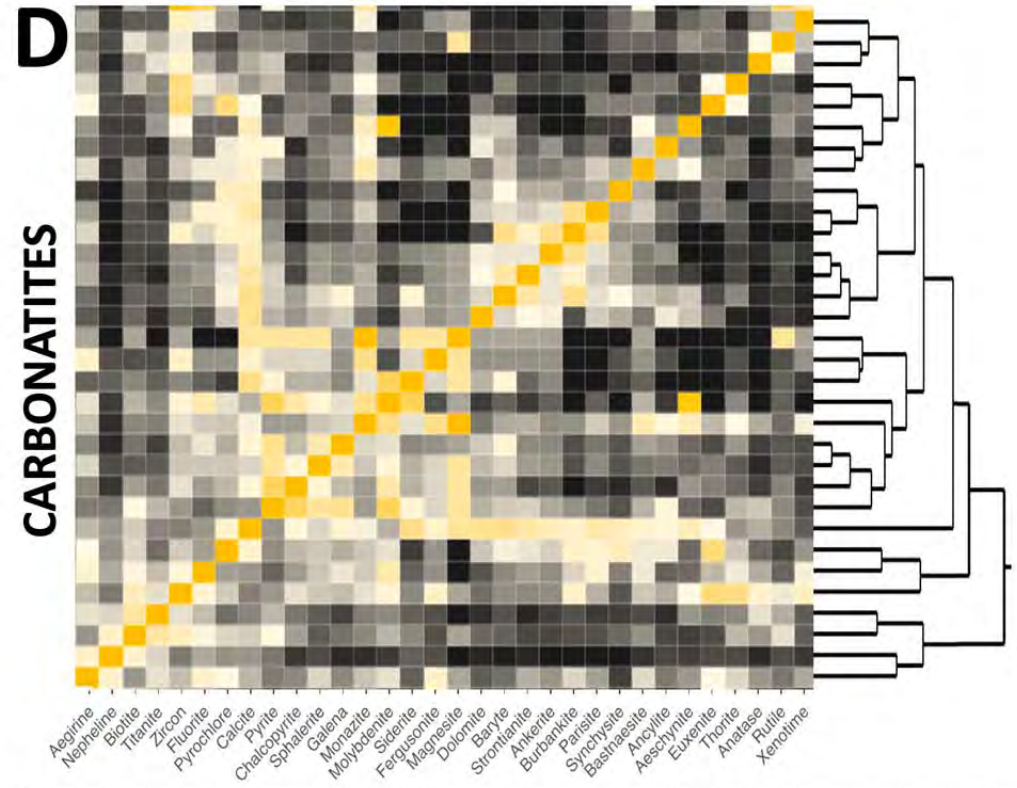

447

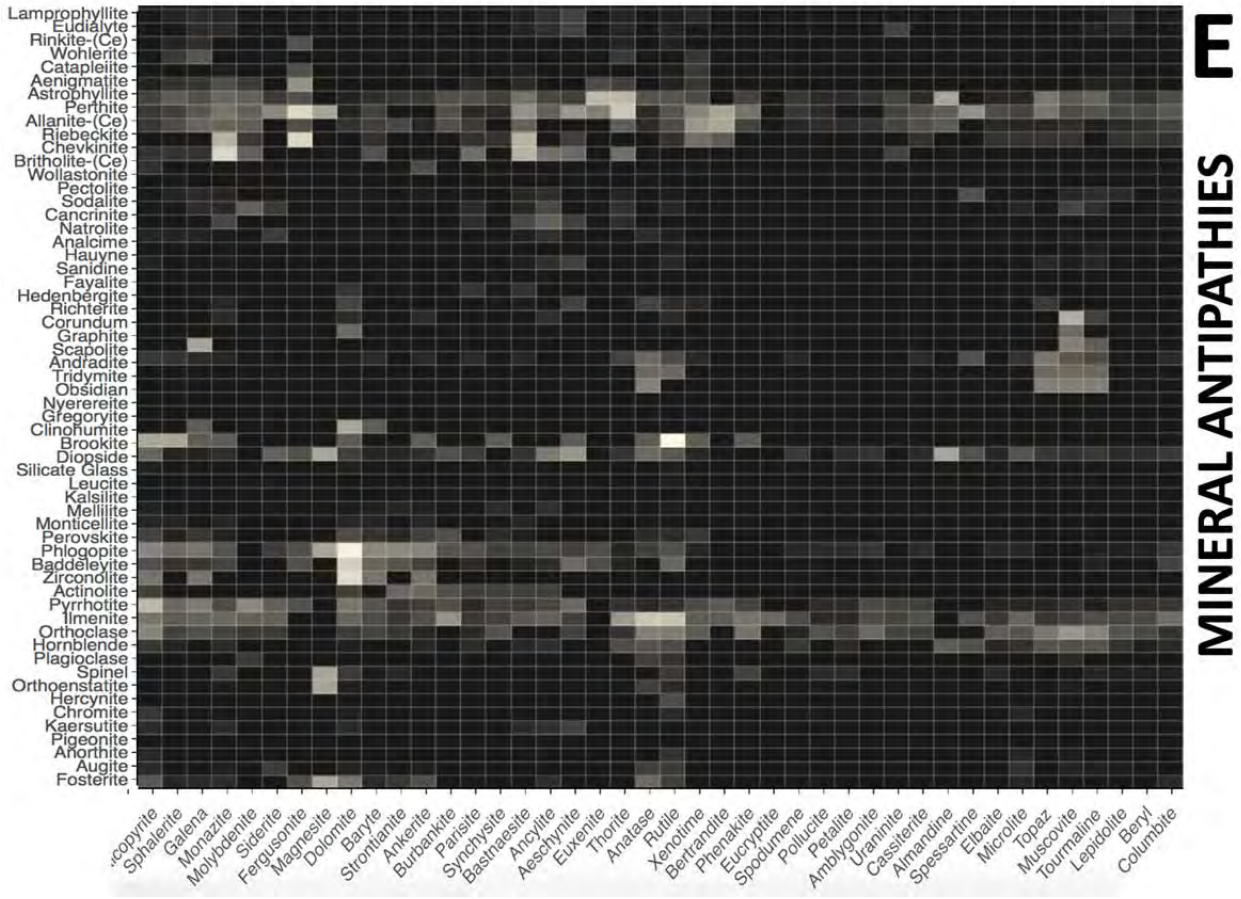

448

This is the peer-reviewed, final accepted version for American Mineralogist, published by the Mineralogical Society of America.
The published version is subject to change. Cite as Authors (Year) Title. American Mineralogist, in press.
DOI: https://doi.org/10.2138/am-2022-8539. http://www.minsocam.org/

Figure 3. Enlargements of features in the heatmap of Figure 2 reveal several groups of closely associated primary igneous minerals, as well as dark regions of mineral "antipathies." **A.** 22 minerals from granites and their rare-element pegmatites are clustered in the upper-righthand corner of Figure 2. All of these Cluster A minerals are also in Community 1 in Figure 1A. **B.** The lower-lefthand section of the heatmap (Figure 2) holds Cluster B with 27 minerals, most of which are typical of mafic rocks; 22 of these minerals also occur in Community 2 (Figure 1A). In addition, a pair of minerals – *fluorapatite* and *magnetite*, which are the two most abundant and widely connected igneous minerals in our study – form their own Cluster F. **C.** Thirty minerals to the lower-left of center in Figure 2 are primarily representative of alkaline igneous rocks; 21 of these Cluster C minerals overlap Community 3 in Figure 1A. An additional two nodes in the extreme lower left of Figure 3C represent the alkali carbonates gregoryite and nyererite (here designated Cluster E), and thus are equivalent to Community 5 in Figure 1A. **D.** Thirty-two minerals of Cluster D to the upper-right of center in Figure 2 are primarily carbonate, sulfide, and other phases associated with carbonatites, and thus largely overlap Community 4 in Figure 1A. **E.** Extensive off-diagonal regions of the heat map in Figure 2 are predominantly black, thus highlighting the large number of mineral antipathies among primary igneous minerals. This 41 x 60 element matrix, enlarged from the lower right of Figure 2, reveals the sparse co-occurrence among minerals from granites or carbonatites (Clusters A and D; 41 columns) with a different set of minerals primarily from ultramafic/mafic and alkaline/agpaitic rocks (Clusters B and C; 60 rows).

Coexistence patterns among the 115 minerals recorded in the heatmap of Figure 2 follow closely the patterns of communities in Figure 1A, albeit with important differences. Compare the four major communities in Figure 1A with the four major clusters in Figures 2 and 3.

Cluster A: Figure 3A is an enlargement of the upper-right corner of Figure 2. This area is a 22 x 22 symmetrical matrix of minerals that form in granites and their associated rare-element pegmatites. All 22 of these Cluster A minerals also occur in Community 1 of Figure 1A. Four additional Community 1 phases – *euxenite*, *thorite*, *xenotime*, and *zircon* – all high-field-strength-element accessory phases that occur frequently in both

This is the peer-reviewed, final accepted version for American Mineralogist, published by the Mineralogical Society of America.
The published version is subject to change. Cite as Authors (Year) Title. American Mineralogist, in press.
DOI: https://doi.org/10.2138/am-2022-8539. http://www.minsocam.org/

complex granite pegmatites and in carbonatites – are shifted to Cluster D (primarily carbonatite minerals) in our heatmap analysis (see below).

Cluster B (and F): A group of 27 minerals occupies a 27 x 27-mineral symmetrical sub-matrix (Figure 3B), which is found in the lower-left corner of the heatmap (Figure 2). This Cluster B of minerals is most typical of silica-undersaturated ultramafic/mafic rocks, with 22 of these phases also occuring in Community 2 of Figure 1A. However, 9 of the 32 minerals in Community 2 of Figure 1A occur in Group C (alkaline igneous suites) in the heatmap analysis – phases designated "2-C" in Table 2. In addition, the two most frequently reported igneous phases in our survey – *fluorapatite* and *magnetite*, which occur frequently in all major igneous rock communities – form their own 2-mineral Cluster F in the extreme lower-left corner of Figure 2.

Cluster C (and E): A subset of 30 minerals, most of which are often associated with alkaline igneous suites, are grouped to the lower-left of center in Figure 2 (Figure 3C). Of these 30 minerals in Cluster C, 21 also occur in Community 3 in Figure 1A. An additional two nodes in the extreme lower left of Figure 3C represent the alkali carbonates *gregoryite* and *nyererite* ("Cluster E"), and thus are equivalent to Community 5 in Figure 1A.

Cluster D: A fourth group of 32 minerals forms a symmetrical sub-matrix to the upper-right of center in Figure 2 (Figure 3D). This well-defined group primarily represents carbonates (13 minerals), sulfides (5 minerals), and other phases associated with carbonatites. Twenty-three of these Cluster D minerals also occur in Community 4 in

This is the peer-reviewed, final accepted version for American Mineralogist, published by the Mineralogical Society of America.
The published version is subject to change. Cite as Authors (Year) Title. American Mineralogist, in press.
DOI: https://doi.org/10.2138/am-2022-8539. http://www.minsocam.org/

Figure 1A. However, 9 other Cluster D minerals are associated with Communities 1, 2, or 3 (designated in Table 2 as "1-D", "2-D", or "3-D").

An important feature of the heatmap in Figure 2 is the delineation of mineral antipathies. Extensive off-diagonal regions of the heatmap are predominantly black, thus highlighting the large number of mineral pairs that rarely or never occur among primary igneous minerals. Figure 3E enlarges a 41 x 60 matrix area from the lower right of Figure 2 – a region that represents the strikingly sparse co-occurrence among 41 minerals from Cluster A and Cluster D (granites or carbonatites ; 41 columns) with a different set of 60 minerals primarily from Cluster B and Cluster C (ultramafic/mafic and alkaline/agpaitic rocks; 60 rows).

Detailed analysis of the thousands of primary igneous mineral pairs that are not observed is beyond the scope of this contribution. However, it is evident that missing mineral pairs arise from both of Bowen's (1928) proposed reasons: "actual incompatibilities … which have a purely chemical basis" (e.g., *forsterite/quartz*), as well as "incompatibilities of a different kind, based wholly on petrogenetic factors" (e.g., *augite/quartz*).

Bipartite network of igneous minerals and their host lithologies: Figure 4 is a bipartite network (i.e., a network with links between two different kinds of nodes) that illustrates 919 diamond-shaped nodes representing primary igneous minerals and their 1410 links to 8 crystal- or volcano-shaped nodes representing different groups of igneous rocks, as first described by Hazen and Morrison (2022) and modified here in Supplementary Table 2. This bipartite network was made using the "visNetwork" (Almende et al. 2021) and "igraph" (Csardi & Nepusz 2006) R packages. The code for construction of this network can be found at:

519 [https://github.com/anirudhprabhu/StellarNet/tree/master/PartVII]. The network layout uses
520 the "barnesHut" approximation algorithm (Barnes and Hut 1986).

521

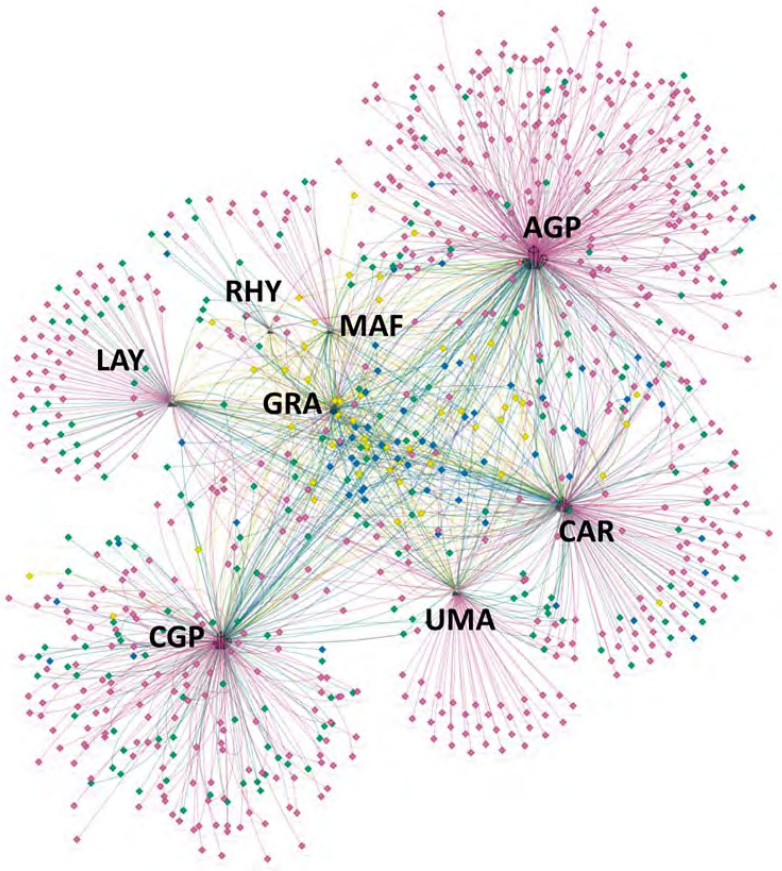

522

523 Figure 4. This bipartite network of 919 primary igneous minerals (colored diamond-shaped nodes)
524 displays 1410 links to 8 icons representing different major groups of igneous rocks, as first described by
525 Hazen and Morrison (2022) and modified here (Supplementary Table 2). Three-letter identifiers are
526 UMA = ultramafic (with 122 minerals); MAF = mafic (75); GRA = granites (99); RHY = rhyolite (38); CGP =
527 rare-element granite pegmatites (296); AGP = alkaline igneous complexes (420); CAR = carbonatites
528 (239); and LAY = layered igneous intrusions (121). Mineral nodes are colored according to relative
529 abundances: 51 blue nodes represent the most common major igneous minerals; 64 yellow nodes
530 represent common accessory minerals; 182 green nodes represent uncommon igneous minerals; and
531 622 pink nodes represent the rarest primary igneous minerals.
532

533 This bipartite network displays several features that are common to other mineral systems
534 (Morrison et al. 2017, 2020, 2022; Hazen et al. 2019). A minority of 83 relatively common
535 minerals (mostly colored blue or yellow in Figure 3) adopt central positions, where they are
536 linked to three or more different groups of igneous minerals. These 83 minerals from multiple
537 igneous lithologies are less diagnostic in defining communities or clusters of closely-related
538 minerals than minerals known from only one type of igneous rock. Only 28 minerals in the core
539 of the bipartite network are linked to 5 or more groups of igneous rocks, with 10 of the most
540 common minerals (all occurring in more than 200 of the 1850 rock modes in Supplementary
541 Table 3) linked to the full range of 8 igneous rock groups: *biotite*, *diopside*, *fluorapatite*,
542 *hornblende*, *ilmenite*, *magnetite*, *microcline*, *orthoclase*, *pyrite*, and *titanite* (Supplementary
543 Table 2).

544 By contrast, a significant majority of minerals are rare (represented by green or pink nodes);
545 678 of these minerals are linked to a single igneous mineral group, thus creating five dramatic
546 "starbursts" of nodes decorating the periphery of the bipartite network. Alkaline igneous
547 complexes boast the greatest number – 249 of these single-node phases, which create the
548 largest such display in the upper right of the network. Granite pegmatites are linked to 205 of
549 these rare minerals, which form a symmetrical fan-shaped array in the lower left of the
550 network. Other starbursts more centrally located are connected to carbonatites (73 minerals),
551 layered igneous complexes (65), and ultramafic rocks (38). Thus, as in many other mineral
552 systems, most primary igneous minerals are rare, known from 5 or fewer localities and formed
553 by a single process (Hazen and Ausubel 2016).

This is the peer-reviewed, final accepted version for American Mineralogist, published by the Mineralogical Society of America.
The published version is subject to change. Cite as Authors (Year) Title. American Mineralogist, in press.
DOI: https://doi.org/10.2138/am-2022-8539. http://www.minsocam.org/

In addition, 158 minerals are associated with exactly two of the 8 igneous rock groups. More than a quarter of these pairings (41 minerals) connect alkaline igneous complexes to carbonatites, which consequently appear adjacent to each other in the network of Figure 4. These 41 shared mineral kinds attest to the close relationship of carbonatites as the final stage in many alkaline igneous complexes. Other strong connections of a mineral to exactly two groups of igneous minerals include ultramafic/carbonatite (20 minerals), granite pegmatite/alkaline rocks (17), granite/alkaline rocks (12), and carbonatite/layered igneous rocks (12). The topology of Figure 4 thus reflects many details of both mineral co-occurrence and their distributions across several kinds of igneous lithologies.

IMPLICATIONS

"*The minerals of which a rock is composed are the expression of a response to the conditions of their genesis.*"

N. L. Bowen, *The Evolution of the Igneous Rocks* (1928, p.321)

Our investigations of the distributions of primary minerals among a worldwide inventory of 1850 varied rocks views igneous petrology and mineralogy from an unusual perspective – at a globally integrated spatial and temporal scale. This broad overview approach, which complements more traditional detailed petrologic studies of individual localized igneous bodies, reinforces long-established concepts in petrology, including numerous mineral associations (as well as antipathies), equilibrium phase relationships, mechanisms and patterns of minor and rare element concentrations, reaction sequences, and liquid lines of descent (e.g., Shand 1943; Carmichael et al. 1973; Philpotts and Ague 2009). But can data-driven approaches to igneous

This is the peer-reviewed, final accepted version for American Mineralogist, published by the Mineralogical Society of America.
The published version is subject to change. Cite as Authors (Year) Title. American Mineralogist, in press.
DOI: https://doi.org/10.2138/am-2022-8539. http://www.minsocam.org/

petrology reveal anything new? We suggest that these mineralogical data embed important relationships that can inform long-standing questions in the field – opportunities that warrant future exploration. Consider three examples.

Embedded phase relationships in networks of primary igneous minerals: Coexistence data in Supplementary Tables 4 and 5 have been extracted from modal analyses of presumably primary minerals in 1850 igneous rocks (Supplementary Table 3), which often preserve equilibrium phase relationships. Therefore, the unipartite network configuration at P = 49 % (Figure 1) records frequently observed links between pairs of minerals, as well as groups of 3 or more links in higher dimensions, that represent equilibrium igneous mineral assemblages (e.g., Figure 1B). We suggest that the observed network topology embeds the corresponding phase equilibrium topologies for numerous multi-component chemical systems of interest to the evolution of igneous rocks.

Detailed phase relationships at low and moderate pressures for many mafic and felsic chemical systems relevant to the major elements of igneous rocks have been well established through more than a century of experimental petrology and thermochemical modeling (e.g., Levin et al. 1964 and subsequent volumes; Yoder 1976; Ghiorso and Sack 1995; Ghiorso et al. 2002; Philpotts and Ague 2009). All of the phase relationships that govern crystallization must be embedded in the topology of the unipartite network of Figure 1. For example, we can detect the continuum of major minerals crystallizing from mafic magmas in Community 2, with the importance of olivine, pyroxene, and calcic plagioclase reflected in their common connectivity.

599 However, detailed phase relationships in systems of higher chemical dimensions relevant to
600 the diversity of natural magma compositions, including phase equilibria that encompass both
601 major and accessory minerals with relatively rare elements, are only poorly determined
602 experimentally. In these instances, observations of igneous rocks themselves can provide us
603 with insights on mineral associations that are not readily obtained in other ways. Therefore, an
604 important direction for future studies includes the identification of high-dimensional igneous
605 phase relationships and, perhaps, extraction of thermochemical parameters relevant to these
606 assemblages.

607 As a prelude to those forthcoming investigations, in Figure 5 we present a unipartite
608 network that includes only the 91 less-frequently encountered minerals – all minerals with
609 fewer than 200 occurrences in Supplementary Tables 2 and 3 – among the 115 primary igneous
610 phases illustrated in Figure 1. Thus, we removed the 24 most common major igneous minerals,
611 all of which incorporate one or more of the commonest cations (Na, K, Mg, Ca, Fe, Al, Ti, and/or
612 Si). Consequently, Figure 5 emphasizes the distribution of many rare-element phases amongst
613 different igneous rock communities. In particular, we wanted to see if the four major
614 communities observed for all minerals persist when the network "glue" of the commonest
615 phases is removed.

This is the peer-reviewed, final accepted version for American Mineralogist, published by the Mineralogical Society of America.
The published version is subject to change. Cite as Authors (Year) Title. American Mineralogist, in press.
DOI: https://doi.org/10.2138/am-2022-8539. http://www.minsocam.org/

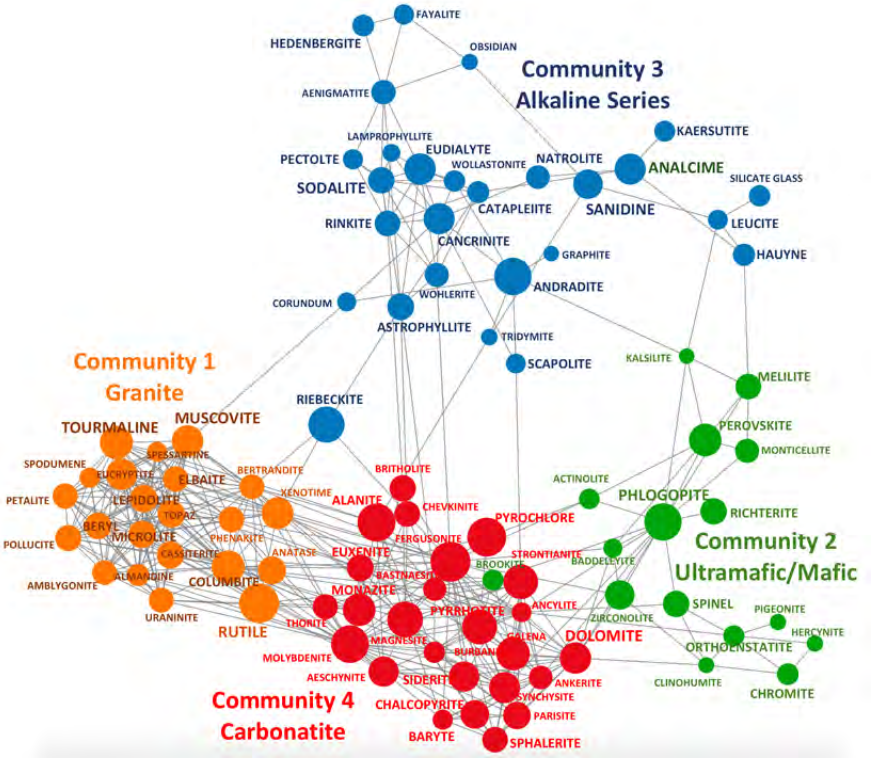

Figure 5. A unipartite network illustrates 453 connections among 91 nodes that represent minor/accessory primary igneous minerals. In this figure, links are drawn between two minerals if at least 26 % of rocks recorded in Supplementary Table 3 that incorporate the less common mineral also incorporate the more common mineral. Louvain community detection defines four sub-equal communities that are equivalent to those of Figure 1A. The size of each node represents its degree centrality, which is equal to the number of links from that node to other nodes. The sizes of the node labels represent the relative abundance of each mineral. An interactive version of this figure is available at: [https://observablehq.com/@anirudhprabhu/evol_sys_part7_unipartite_minor_minerals]. Hover your cursor over any node to identify the corresponding mineral; click and hold your cursor to move that node to identify links to other nodes; use your cursor to move the "Weight Threshold" vernier to systematically eliminate links between nodes based on *P* values (see text).

Links in Figure 5 are drawn between two minerals if at least 26 % of rocks in Supplementary Table 3 that incorporate the less common mineral also incorporate the more common mineral (i.e., P = 26 %; note that at P = 27 %, one mineral, *hedenbergite*, is no longer connected). The

resulting network, with 453 out of a possible 4095 links, is significantly less dense (D = 0.11) than the corresponding network at P = 0.26 in Figure 1. [Figure 5 is a static rendering of a dynamic interactive network (see Figure 5 caption for instructions); for the interactive version go to:

https://observablehq.com/@anirudhprabhu/evol_sys_part7_unipartite_minor_minerals.]

Nevertheless, application of Louvain community detection methods to this network reveals 4 communities that overlap almost completely with those in Figure 1A. This result suggests that well-known trends in the distribution of major rock-forming igneous minerals extend to minor and accessory phases, as well. We conclude that these phases, though typically volumetrically insignificant, are equally diagnostic of different igneous lithologies.

Two aspects of Figure 5 deserve further study. First, previous studies have demonstrated that Bowen's reaction series is embedded in the network of major rock-forming igneous minerals (Morrison et al. 2017; their Figure 2B). Figure 5 expands on this work, pointing to the liklihood that Bowen's classic reaction series, based on crystallization sequences of major mafic and feldspar group minerals, might be extended to the sequence of crystallization of minor/accessory minerals that incorporate rare elements.

A second feature of Figure 5 is the distinctive separation of the minerals in the several communities. For example, Community 1, which represents granites and other quartz-bearing lithologies, is unconnected to Community 2, which represents ultramafic/mafic lithologies. Though based on minor and accessory minerals, most of which incorporate rare elements, this Figure 5 separation appears to correspond to the well-documented "Daly gap," as typically illustrated on a major-element "FMA" (Fe-Mg-Alkali) ternary diagram (Daly 1925; Chayes 1963;

Bonnefoi et al. 1995; Philpotts and Ague 2009). The Daly gap reflects the paucity of rocks of intermediate SiO_2 compositions in suites of mafic and felsic igneous rocks, as manifest in bimodal distributions of lithologies. We suggest that this compositional feature can be extended to minor elements and their minerals, as well. If so, then the significant separations between Communities 2 and 3, as well as between 3 and 4 could, represent compositional gaps analogous to the Daly gap.

The genesis of carbonatites: The topologies of Figures 1, 2, and 3, and in particular the close parallels among the major mineral Communities (1 to 4) and Clusters (A to D), have the potential to inform models of igneous magma descent. One of the most striking (and to us unexpected) findings of this study is the strong grouping of 115 primary igneous minerals into four distinct communities or clusters (Figures 1, 2, 3, and 5). One plausible conclusion is that Communities 1 through 4 in Figures 1A and 5, and, equivalently, Clusters A to D, in Figures 2 and 3, arise from 4 genetically distinct types of magmas.

Consider the example of granite formation. We initially speculated that, in spite of the Daly gap, a continuum of rock types, compositions, and mineralogies would span the range from silica-undersaturated ultramafic rocks, through mafic, intermediate, and ultimately granitic lithologies and their rare-element pegmatites. Instead, we observe relatively sharp divides, with the great majority of minerals in Community 1 (ultramafic, mafic, and intermediate rocks) almost never found in granitic rocks of Community 2 (see Figure 3E), and *vice versa*. These orthogonal relationships, reflecting the strong antipathies between most minerals of Community 1 and Community 2, are consistent with the observation that most granitic rocks do

676 not represent the final stages of a continuous crystallization sequence of more mafic lithologies
677 (e.g, "M"-type granites; Whalen 1985; Philpotts and Ague 2009). Rather, the majority of
678 granites are "I"- and "S"-types (Chappell and White 1974, 2001); they and their pegmatites
679 appear to be separately derived primarily by partial melting of other lithologies – igneous or
680 sedimentary, respectively. Note, however, that a spectrum of sources, including primary
681 magmas and/or their differentiates, country rock contamination, and partial melting of crustal
682 lithologies, may contrubute in any given granite (Ague and Brimhall 1988; Annen et al. 2006;
683 Jagoutz and Klein 2018; Tassara et al. 2021).

684 Similarly, it was perhaps reasonable to expect a continuous mineralogical transformation
685 from felsic alkaline rocks with more silica, to nepheline syenites, agpaitic rocks, and ultimately
686 carbonatites. In their survey of the world's carbonatites, Woolley and Kjardgaard (2006) note
687 that most examples of carbonatites (74 %) are closely associated with ultrabasic and alkaline
688 rocks, often with carbonatites occurring as the volumetrically minor core of a highly
689 fractionated igneous complex. These observations point to two possible origin processes: (1) via
690 late-stage fractionation, or (2) by segregation of an immiscible C-rich fluid. However, many
691 other carbonatites appear to originate as direct C-rich, Si-poor partial melts from the mantle
692 (Yaxley and Brey 2004; Yaxley et al 2021) and a debate continues regarding the origin of
693 carbonatitic magmas, in particular the degree to which they derive from primary mantle melts,
694 as opposed to late-stage fractionated magmas from alkaline complexes (Kamenetsky et al 2021;
695 Yaxley et al 2021).

696 Our community detection analyses reveal a significant divide between feldspathoid-bearing
697 alkaline igneous suites and carbonatites (Figures 1 and 5), most strikingly displayed in the

almost complete absence of any silicate minerals in the carbonatite groupings of minerals, as well as many other mineral antipathies (see Figure 3E). The carbonatites in our mineralogical survey include most of the examples cited by Woolley and colleagues (Woolley 1987, 2001, 2019; Kogarko et al. 1995), and therefore are mostly associated with the final stages of alkaline igneous complex evolution. It is intriguing, therefore, that a distinct divide occurs between Communities 3 and 4 of Figure 1A, as well as a corresponding break between Clusters C and D in Figures 2 and 3. Such topological discontinuities may point to the production of immiscible C-rich fluids in the case of most alkaline igneous complexes (e.g., Kjarsgaard et al. 1995; Weidendorfer et al. 2016), as well as mantle-derived carbonatite melts (Dasgupta et al. 2004; Foley et al 2009). A promising follow-up to this study, therefore, might be to apply these analytical and visualization approaches separately to the ~450 carbonatites associated with alkaline igneous complexes, in comparison to the ~150 other carbonatites, as summarized in the work of Woolley and colleagues.

<u>*The evolution of the igneous minerals*</u>:

> "*The use of the term 'evolution' in the title is intended to designate only a process of derivation of rocks from a common source and not to imply that detailed knowledge of the process which the term connotes when applied to organic development*."
>
> N. L. Bowen, *The Evolution of the Igneous Rocks* (1928, "Preface")

Bowen (1928) was well aware that his use of the word "evolution" in a treatise on petrology was unconventional and quite different from its more familiar context in evolutionary biology. He modestly adopted the term in his title to imply nothing more than a temporal sequence of rock and mineral-forming events. With the exception of a brief explanation in the "Preface" of

his 332-page book, and a few scattered uses of the phrase "thermal evolution," Bowen seems to have asiduously avoided further references to "evolution" in his text.

Our investigations of the evolution of the igneous rocks suggest that Bowen could have taken a bolder stance. Igneous minerals have not only changed congruently through Earth's 4.566-billion-year history, as he implies, but they have also displayed another striking characteristic of many evolving chemical systems: minerals have dramatically increased in diversity and in complexity through the first two billion years of Earth history (Krivovichev et al. 2018).

We speculate that Earth's earliest igneous lithologies, commencing more than 4.56 billion years ago, were ultramafic rocks rich in olivine and/or pyroxene – rocks that have been present throughout the planet's history (Morrison et al. 2022). We identify 122 mineral kinds associated with these silica-undersaturated rocks (Supplementary Table 2).

We further suggest that basalt, gabbro, and other mafic rocks with significant calcic plagioclase, which were formed from magmas primarily derived by decompression melting of ultramafic rocks, have been present almost as long as ultramafics, probably by 4.56 Ga. With mafic rocks, the number of primary igneous minerals increased to 166.

Small volumes of quartz-normative igneous rocks, including M-type granites, probably formed during the final crystallization stages of some gabbroic intrusions prior to 4.5 Ga. However, much greater volumes of granitoid rocks, including continental arc tonalite-trondhjemite-granordiorite (TTG) suites and true granites, as well as their eruptive equivalents (rhyolite and dacite, for example), were likely initially formed by partial melting of basalt and/or sediments (e.g., Rollinson 2007), possibly by 4.4 Ga based on suggestive inclusions of quartz

744 and muscovite in Hadean zircons (Maas et al. 1992; Harrison 2009; Harrison et al. 2017; though
745 see Burnham and Berry 2017). Formation of granitic rocks further expanded Earth's repertoire
746 of igneous minerals to at least 246 known kinds. All of these presumed Hadean lithologies could
747 have arisen before the advent of plate tectonics.

748 Four distinctive groups of igneous rocks – complex granite pegmatites, alkaline igneous
749 suites, carbonatites, and layered igneous intrusions, each of which contains diagnostic
750 concentrations of rare elements – significantly postdate the igneous lithologies outlined above.
751 All appear to have first formed close to ~3.0 Ga, possibly because they required the extensive
752 fluid-rock interactions of the crust and upper mantle associated with subduction (although
753 significant debates persist concerning the commencement, style, and rates of subduction on
754 early Earth; e.g., Sizova et al. 2010, 2014; Johnson et al., 2017; Wan et al. 2020; Korenaga, 2021;
755 Mitchell et al., 2022). Each of these four types of exotic igneous mineralization added to the
756 diversity, as well as the chemical and structural complexity, of Earth's minerals.

757 Layered igneous intrusions with extreme enrichments in PGEs, as well as Au, Cu, and other
758 metals, appear as early as 2.8 Ga (O'Driscoll and Van Tongeren 2017). They added 66 mineral
759 kinds, mostly sulfides, arsenides, and sulfosalts, to Earth's mineral inventory.

760 Complex granite pegmatites, typically with extreme enrichments in light lithophile elements
761 (Li, Be, B), also first appeared no more than 3 billion years ago (London 2008). These deposits
762 hold at least 296 different minerals, 205 of which are only recorded from granite pegmatites.

763 A similar diversity of rare-element minerals is hosted by a range of silica-undersaturated
764 alkaline igneous rocks, notably the rare suites of minerals associated with agpaitic rocks. We

765 record a remarkable 420 different mineral kinds from alkaline complexes, of which 249
766 minerals, many that concentrate high-field-strength elements, are unique to these lithologies.

767 The fourth group of exotic igneous rocks are the carbonatites, which feature one or more
768 carbonate minerals as major phases. The earliest known examples occurred ~3.0 Ga (Woolley
769 1987, 2001, 2019; Kogarko et al. 1995; Bizzarro et al. 2002; Wooley and Kjarsgaard 2008; Jones
770 et al. 2013; Kamenetsky et al 2021), and they have been frequent, if highly localized, features of
771 the crust ever since. Their complement of 239 mineral kinds includes 73 minerals unique to
772 carbonatites, with numerous rare element accessory minerals of REEs and HFSEs
773 (Chakhmouradian 2006; Simandl and Paradis 2018; Anenburg et al. 2021; Christy et al. 2021).
774 With the possible exception of unusual alkali carbonatites, which quickly alter and thus have
775 been lost in the deep-time rock record (Zaitsev and Keller 2006), there appear to have been no
776 new groups of igneous rocks since the late Archean Eon.

777

778 Stepping back from these specific considerations, a larger message of this study is the great
779 potential for data-driven discovery in mineralogy and petrology. More than a century of
780 research has produced a prodigious amount of data on igneous rocks – countless millions of
781 mineral analyses from countless thousands of rocks. Keys to progress are the significant
782 numbers of attributes associated with rocks and their constituents: scores of trace and minor
783 elements; hundreds of stable isotopes; varied solid and fluid inclusions; optical, electrical,
784 magnetic, and elastic properties; twinning and exsolution; and rock textures, fabrics, and grain
785 morphologies. Those data hold the promise of "abductive" discoveries: the assurance that as
786 yet unseen patterns reside in the analysis of multi-dimensional systems (Hazen 2014). Armed

787 with a growing arsenal of data resources, analytical methods, and visualizations, we eagerly
788 anticipate this new era of Earth materials informatics.

789

790 **ACKNOWLEDGMENTS**

791 We are especially grateful to Jay Ague, Robert Downs, George Harlow, and Michael Wong
792 for valuable discussions and reviews of an early version of this contribution. We also thank
793 Associate Editor Steven Simon, and reviewers Mark Ghiorso and Ross Mitchell for their
794 thorough, thoughtful, and constructive reviews.

795

796 **FUNDING**

797 Studies of mineral evolution and mineral ecology have been supported by the Alfred P.
798 Sloan Foundation, the W. M. Keck Foundation, the John Templeton Foundation, the NASA
799 Astrobiology Institute ENIGMA team, a private foundation, and the Carnegie Institution for
800 Science. Any opinions, findings, or recommendations expressed herein are those of the authors
801 and do not necessarily reflect the views of the National Aeronautics and Space Administration.

802

REFERENCES

Ague, J.J., and Brimhall, G.H. (1988) Magmatic arc asymmetry and distribution of anomalous plutonic belts in the batholiths of California: effects of assimilation, crustal thickness, and depth of crystallization. Geological Society of America Bulletin, 100, 912-927.

Almende, B.V., and Contributors, Benoit Thieurmel and Titouan Robert (2021). visNetwork: Network Visualization using 'vis.js' Library. R package version 2.1.0. https://CRAN.R-project.org/package=visNetwork.

Anenburg, M., Broom-Fendley, S., and Chen, W. (2021) Formation of rare earth deposits in carbonatites. Elements, 17, 327-332.

Annen, C., Blundy, J.D., and Sparks, R.S.J. (2006) The genesis of intermediate and silicic magmas in deep crustal hot zones. Journal of Petrology, 47, 505-539.

Anthony, J.W., Bideaux, R.A., Bladh, K.W., and Nichols, M.C. (1990-2003) Handbook of Mineralogy, 6 volumes. Mineral Data Publishing.

Armbruster, T., Bonazzi, P., Akasaka, M., Bermanec, V., Chopin, C., Gieré, R., Heuss-Assbichler, S., Liebscher, A., Menchetti, S., Pan, Y., and Pasero, M. (2006) Recommended nomenclature of the epidote-group minerals. European Journal; of Mineralogy, 18, 551-567.

Atencio, D., Andrade, M.B., Christy, A.G., Gieré, R., and Kartashov, P.M. (2010) The pyrochlore supergroup of minerals: Nomenclature. Canadian Mineralogist, 48, 673-698.

Badro, J., and Walter, M. [Eds.] (2015) The Early Earth: Accretion and Differentiation. American Geophysical Union Geophysical Monograph, 212.

Barnes, J., and Hut, P. (1986) A hierarchical O(*N* log *N*) force-calculation algorithm. Nature, 324, 446-449.

Berdnikov, N., Kepezhinskas, P., Konovalova, N., and Kepezhinskas, N. (2022) Formation of gold alloys during differentiation of convergent zone magmas: Constraints from an Au-rich websterite in the Stanovoy suture zone (Russian Far East). Geosciences, in press.

Bird, A., and Tobin, E. (2015) Natural Kinds. In Zalta, E.N. (ed.) The Stanford Encyclopedia of Philosophy (Spring 2015 Edition) https://plato.stanford.edu/entries/natural-kinds/

Bizzarro, M., Simonetti, A., Stevenson, R.K., and David, J. (2002) Hf isotope evidence for a hidden mantle reservoir: Geology, 30, 771-774.

Blondel, V.D., Guillaume, J.-L., Lambiotte, R., and Lefebvre, E. (2008) Fast unfolding of communities in large networks. Journal of Statistical Mechanics, 2008, 1–12.

Bonnefoi, C.C., Provost, A., and Albarede, F (1995) The “Daly gap” as a magmatic catastrophe. Nature, 378, 270-272.

Bostock, M., Ogievetsky, V., and Heer, J. (2011). D^3 data-driven documents. IEEE transactions on visualization and computer graphics, 17(12), 2301-2309.

Boujibar, A., Howell, S., Zhang, S., Hystad, G., Prabhu, A., Liu, N., Stephan, T., Narkar, S., Eleish, A., Morrison, S.M., Hazen, R.M., and Nittler, L.R. (2021) Cluster analysis of presolar silicon carbide grains: Evaluation of their classification and astrophysical implications. Astrophysical Journal Letters. DOI: 10.3847/2041-8213/abd102

Bowen, N.L. (1912, 1913) The order of crystallization in igneous rocks. Journal of Geology, 20, 457-468; 21, 399-401.

Bowen, N.L. (1915) Evolution of igneous rocks. Carnegie Institution of Washington Year Book, 15, 144-145.

Bowen, N.L. (1922) The reaction principle in petrogenesis. Journal of Geology, 30, 177-198.

847 Bowen, N.L. (1927) The origin of ultrabasic and related rocks. American Journal of Science, 14,
848 89-108.
849 Bowen, N.L. (1928) The Evolution of the Igneous Rocks. Princeton University Press.
850 Bowles, J.F.W., Howie, R.A., Vaughan, D.J., and Zussman, J. (2011) Rock-Forming Minerals.
851 Volume 5A, Second Edition. Non-Silicates: Oxides, Hydroxides and Sulfides. The Geological
852 Society of London.
853 Boyd, R. (2010) Homeostasis, higher taxa, and monophyly. Philosophical Science, 77, 686-701.
854 Bradley, D.C. (2011) Secular trends in the geologic record and the supercontinent cycle. Earth
855 Science Reviews, 108, 16-33.
856 Burke, E.A.J. (2006) The end of CNMMN and CCM—Long live the CNMNC! Elements, 2, 388.
857 Burnham, A.D., and Berry, A.J. (2017) Formation of Hadean granites by melting of igneous crust:
858 Nature Geoscience, 10, 457-461.
859 Carmichael, I.S.E., Turner, F.J., and Verhoogen, J. (1973) Igneous Petrology. McGraw-Hill Book
860 Company.
861 Castle, R.O., and Lindsley, D.H. (1993) An exsolution silica-pump model for the origin of
862 myrmekite. Contributions to Mineralogy and Petrology, 115, 58-65.
863 Chakhmouradian, A.R. (2006) High-field-strength elements in carbonatitic rocks: geochemistry,
864 crystal chemistry, and significance for constraining the sources of carbonatites. Chemical
865 Geology, 235, 138-160.
866 Chang, L.L.Y., Howie, R.A., and Zussman, J. (1996) Rock-Forming Minerals. Volume 5B, Second
867 Edition. Sulphates, Carbonates, Phosphates and Halides. Longman Group.

868 Chappell, B.W., and White, A.J.R. (1974) Two contrasting granite types. Pacific Geology, 8, 173-
869 174.

870 Chappell, B.W., and White, A.J.R. (2001) Two contrasting granite types: 25 years later.
871 Australian Journal of Earth Sciences, 48, 489-499.

872 Chayes, F. (1963) Relative abundance of intermediate members of the oceanic basalt-trachyte
873 association. Journal of Geophysical Research, 68, 1519-1534.

874 Chiama, K., Gabor, M., Lupini, I., Rutledge, R., Nord, J.A., Zhang, S., Boujibar, A., Morrison, S.M.,
875 and Hazen, R.M. (2020) Garnet: A comprehensive standardized database of garnet
876 geochemical analyses integrating provenance and paragenesis. Geological Society of
877 America Annual Meeting 2020, 52. Doi: 10.1130/abs/2020AM-354256.

878 Chiama, K., Gabor, M., Lupini, I., Rutledge, R., Nord, J.A., Zhang, S., Boujibar, A., Bullock, E.S.,
879 Walter, M.J., Spear, F., Morrison, S.M., and Hazen, R.M. (2022) ESMD-Garnet dataset. Open
880 Data Repository, https://doi.org/10.48484/camh-xy98

881 Christy, A.G., and Atencio, D. (2013) Clarification of status of species in the pyrochlore
882 supergroup. Mineralogical Magazine, 77, 13-20.

883 Christy, A.G., Pekov, I.V., and Krivovichev, SV. (2021) The distinctive mineralogy of carbonatites.
884 Elements, 17, 333-338.

885 Cleland, C.E., Hazen, R.M., and Morrison, S.M. (2021) Historical natural kinds in mineralogy:
886 Systematizing contingency in the context of necessity. Proceedings of the National Academy
887 of Sciences, 108, e2015370118 (8 p.)

888 Csardi, G., and Nepusz, T. (2006) The igraph software package for complex network research.
889 InterJournal, Complex Systems, 1695. https://igraph.org

Daly, R.A. (1925) The geology of Ascension Island. Proceedings of the American Academy of Arts and Sciences, 60, 1-80.

Dasgupta, R., Hirschmann, M.M., and Withers, A.C. (2004) Deep global cycling of carbon constrained by the solidus of anhydrous carbonated eclogite under mantle conditions. Earth and Planetary Science Letters, 227, 73-85.

Deer, W.A., Howie, R.A., and Zussman, J. (1982-2013) Rock-Forming Minerals. Second Edition. 11 volumes. Longman, John Wiley, and The Geological Society of London.

Deer, W.A., Howie, R.A., and Zussman, J. (1982) Rock-Forming Minerals. Volume 1A, Second Edition. Orthosilicates. Longman.

Deer, W.A., Howie, R.A., and Zussman, J. (1986) Rock-Forming Minerals. Volume 1B, Second Edition. Disilicates and Ring Silicates. John Wiley.

Deer, W.A., Howie, R.A., and Zussman, J. (1997a) Rock-Forming Minerals. Volume 2A, Second Edition. Single-Chain Silicates. The Geological Society of London.

Deer, W.A., Howie, R.A., and Zussman, J. (1997b) Rock-Forming Minerals. Volume 2B, Second Edition. Double-Chain Silicates. The Geological Society of London.

Deer, W.A., Howie, R.A., and Zussman, J. (2001) Rock-Forming Minerals. Volume 4A, Second Edition. Framework Silicates: Feldspars. The Geological Society of London.

Deer, W.A., Howie, R.A., Wise, W.S., and Zussman, J. (2004) Rock-Forming Minerals. Volume 4B, Second Edition. Framework Silicates: Silica Minerals, Feldspathoids and the Zeolites. The Geological Society of London.

Deer, W.A., Howie, R.A., and Zussman, J. (2009) Rock-Forming Minerals. Volume 3B, Second Edition. Layered Silicates Excluding Micas and Clay Minerals. The Geological Society of

912 London.

913 Dobrzhinetskaya, L.F., Wirth, R., Yang, J., Hutcheon, I.D., Weber, P.K., and Green, H.W. III (2009)
914 High-pressure highly reduced nitrides and oxides from chromitite of a Tibetan ophiolite.
915 Proceedings of the National Academy of Sciences USA, 106, 19233-19238.

916 Elliott, H.A.L., Wall, F., Chakhmouradian, A.R., Siegfried, P.R., Dahlgren, S., Weatherley, S., Finch,
917 A.A., Marks, M.A.W., Dowman, E., and Deady, E. (2018) Fenites associated with carbonatite
918 complexes: a review. Ore Geology Reviews, 93, 38-59.

919 Ewing, R.C. (1976) A numerical approach toward the classification of complex, orthorhombic,
920 rare-earth, AB_2O_6-type Nb-Ta-Ti oxides. Canadian Mineralogist, 14, 111-119.

921 Fleet, M.E. (2003) Rock-Forming Minerals. Volume 3A, Second Edition. Sheet Silicates: Micas.
922 The Geological Society of London.

923 Foley, S.F., Yaxley, G.M., Rosenthal, A., Buhre, S., Kiseeva, E.S., Rapp, R.P., and Jacob, D.E.
924 (2009) The composition of near-solidus melts of peridotite in the presence of CO_2 and H_2O
925 between 40 and 60 kbar. Lithos, 112, Supplement 1, 274-283.

926 Fortunato, S. (2010) Community detection in graphs. Physics Reports, 486, 75-174.

927 Gaines, R.V., Skinner, C., Foord, E.E., Mason, B., and Rosenzweig, A. (1997) Dana's New
928 Mineralogy. John Wiley & Sons.

929 Galili, T., O'Callaghan, A., Sidi, J., and Sievert, C. (2018) Heatmaply: An R package for creating
930 interactive cluster heatmaps for online publishing. Bioinformatics, 34, 1600-1602.

931 Ghiorso, M.S., and Sack, R.O. (1995) Chemical mass transfer in magmatic processes IV. A revised
932 and internally consistent thermodynamic model for the interpolation and extrapolation of

liquid-solid equilibria in magmatic systems at elevated temperatures and pressures. Contributions to Mineralogy and Petrology, 119, 197-212.

Ghiorso, M.S., Hirschmann, M.M., Reiners, P.W., and Kress, V.C. III (2002) The pMELTS: A revision of MELTS for improved calculation of phase relations and major element partitioning related to partial melting of the mantle to 3 GPa. Geochemistry, Geophysics, Geosystems, 3, 1-35.

Girvan, M., and Newman, M.E.J. (2002) Community structure in social and biological networks. Proceedings of the National Academy of Sciences USA, 99, 7821-7826.

Gregory, D.D., Cracknell, M.J., Large, R.R., McGoldrick, P., Kuhn, S., Maslennikov, V.V., Baker, M.J., Fox, N., Belousov, I., Figueroa, M.C., Steadman, J.A., Fabris, A.J., and Lyons, T.W. (2019) Distinguishing ore deposit type and barren sedimentary pyrite using laser ablation-inductively coupled plasma-mass spectrometry trace element data and statistical analysis of large data sets. Economic Geology, 114, 771-786.

Grew, E.S. and Hazen, R.M. (2014) Beryllium mineral evolution. American Mineralogist, 99, 999-1021.

Griffin, W.L., Huang, J.-X., Thomassot, E., Gain, S.E.M., Toledo, V., and O'Reilly, S.Y. (2018) Super-reducing conditions in ancient and modern volcanic systems: sources and behaviours of carbon-rich fluids in the lithospheric mantle. Mineralogy and Petrology, 112, S101-S114.

Guilbert, J.M., and Park, C.F., Jr. (2007) The Geology of Ore Deposits. Waveland Press.

Harker, A. (1964) Harker's Petrology for Students, Eighth Edition Revised by C. R. Tilley, S. R. Nockolds, M. Black. Cambridge University Press.

954 Harrison, T.M. (2009) The Hadean crust: Evidence from > 4 Ga zircons. Annual Reviews of Earth
955 and Planetary Sciences, 37, 479-505.
956 Harrison, T.M., Bell, E.A., and Boehnke, P. (2017) Hadean zircon petrochronology. Reviews in
957 Mineralogy & Geochemistry, 83, 329-363.
958 Hawley, K., and Bird, A. (2011) What are natural kinds? Philosophical Perspectives, 25, 205-221.
959 Hawthorne, F.C., Oberti, R., Harlow, G.E., Maresch, W.V., Martin, R.F., Schumacher, J.C., and
960 Welch, M.D. (2011) Nomenclature of the amphibole supergroup. American Mineralogist, 97,
961 2031-2048.
962 Hazen, R.M. (2014) Data-driven abductive discovery in mineralogy. American Mineralogist, 99,
963 2165-2170.
964 Hazen, R.M. (2019) An evolutionary system of mineralogy: Proposal for a classification based on
965 natural kind clustering. American Mineralogist, 104, 810-816.
966 Hazen, R.M., and Ausubel, J.H. (2016) On the nature and significance of rarity in mineralogy.
967 American Mineralogist, 101, 1245-1251.
968 Hazen, R.M., and Morrison, S.M. (2020) An evolutionary system of mineralogy, Part I: stellar
969 mineralogy (>13 to 4.6 Ga). American Mineralogist, 105, 627-651.
970 Hazen, R.M., and Morrison, S.M. (2021) An evolutionary system of mineralogy, Part V:
971 Planetesimal Aqueous and thermal alteration of planetesimals (4.565 to 4.550 Ga). American
972 Mineralogist, 106, 1388-1419. https://doi.org/10.2138/am-2021-7760
973 Hazen, R.M., and Morrison, S.M. (2022) On the paragenetic modes of minerals: A mineral
974 evolution perspective. American Mineralogist, 107, 1262-1287.

975 Hazen, R.M., Liu, X.-M., Downs, R.T., Golden, J.J., Pires, A.J., Grew, E.S., Hystad, G., Estrada, C.,
976 and Sverjensky, D.A. (2014) Mineral evolution: Episodic metallogenesis, the supercontinent
977 cycle, and the coevolving geosphere and biosphere. Society of Economic Geologists Special
978 Publication, 18, 1-15.
979 Hazen, R.M., Downs, R.T., Elesish, A., Fox, P., Gagné, O., Golden, J.J., Grew, E.S., Hummer, D.R.,
980 Hystad, G., Krivovichev, S.V., Li, C., Liu, C., Ma, X., Morrison, S.M., Pan, F., Pires, A.J., Prabhu,
981 A., Ralph, J., Runyon, S.E., and Zhong, H. (2019) Data-driven discovery in mineralogy: Recent
982 advances in data resources, analysis, and visualization. China Engineering, 5, 397-405.
983 Hazen, R.M., Morrison, S.M., and Prabhu, A. (2021) An evolutionary system of mineralogy, Part
984 III: Primary chondrule mineralogy (4.566 to 4.561 Ga). American Mineralogist, 106, 325-350.
985 Hazen, R.M., Morrison, S.M., Krivovichev, S.L., and Downs, R.T. (2022) Lumping and splitting:
986 Toward a classification of mineral natural kinds. American Mineralogist, 107, 1288-1301.
987 Henry, D.J., Novak, M., Hawthorne, F.C., Ertl, A., Dutrow, B.L., Uher, P., and Pezzotta, F. (2011)
988 Nomenclature of the tourmaline-supergroup minerals. American Mineralogist, 96, 895-913.
989 Hystad, G., Boujibar, A., Liu, N., Nittler, L.R., and Hazen, R.M. (2021) Evaluation of the
990 classification of presolar silicon carbide grains using consensus clustering with resampling
991 methods: an assessment of the confidence of grain assignments. Monthly Notices of the
992 Royal Astronomical Society, 510, 334-350.
993 Jagoutz, O., and Klein, B. (2018) On the importance of crystallization-differentiation for the
994 generation of SiO2-rich melts and the compositional build-up of ARC (and continental) crust.
995 American Journal of Science, 318, 29-63.

Johannsen, A. (1932) A Descriptive Petrography of the Igneous Rocks. Volume II. The Quartz-Bearing Rocks. The University of Chicago Press.

Johannsen, A. (1937) A Descriptive Petrography of the Igneous Rocks. Volume III. The Intermediate Rocks. The University of Chicago Press.

Johannsen, A. (1938) A Descriptive Petrography of the Igneous Rocks. Volume IV. Part I: The Feldspathoid Rocks. Part II: The Peridotites and Perknites. The University of Chicago Press.

Johnsen, O., and Grice, J.D. (1999) The crystal chemistry of the eudialyte group. Canadian Mineralogist, 37, 865-891.

Johnson, T.E., Brown, M., Gardiner, N.J., Kirkland, C.L., and Smithies, R.H. (2017) Earth's first stable continents did not form by subduction: Nature, 543, 239-242.

Jones, A.P., Genge, M., and Carmody, L. (2013) Carbonate melts and carbonatites. Reviews in Mineralogy & Geochemistry, 75, 289-322.

Kamenetsky, V.S., Doroshkevich, A.G., Elliott, H.A.L., and Zaitsev, A.N. (2021) Elements, 17, 307-314.

Kapustin, Y.L. (2010) Features of fenitization around carbonatite bodies. International Geology Review, 25, 1939-1404.

Kjarsgaard, B.A., Hamilton, D.L., and Peterson, T.D. (1995) Peralkaline nepheline/carbonatite liquid immiscibility: comparison of phase compositions in experiments and natural lavas from Oldoinyo Lengai. In: K. Bell and J. Keller [Eds], Carbonatite Volcanism: Oldoinyou Lengai and the Petrogenesis of Natrocarbonatites. Springer-Verlag, pp. 163-190.

Kogarko, L.N., Kononova, V.A, Orlova, M.P., and Woolley, A.R. (1995) Alkaline Rocks and Carbonatites of the World. Part Two: Former USSR. Chapman & Hall.

1018 Korenaga, J. (2021) Hadean geodynamics and the nature of early continental crust. Precambrian
1019 Research, 359, 106178 (28 p.).
1020 Krivovichev, S.V., Krivovichev, V.G., and Hazen, R.M. (2018) Structural and chemical complexity
1021 of minerals: correlations and time evolution. European Journal of Mineralogy, 30, 231-236.
1022 Kutyrev, A., Zelenski, M., Nekrylov, N., Savelyev, D., Kontonikas-Charos, A., and Kamenetsky,
1023 V.S. (2021) Noble metals in arc basaltic magmas worldwide: a case study of modern and pre-
1024 historic lavas of the Tolbachik volcano, Kamchatka. Frontiers of Earth Sciences,
1025 https://doi.org/10.3389/feart.2021.791465.
1026 Laporte, J. (2004) Natural Kinds and Conceptual Change. Cambridge University Press.
1027 Le Bas, M.J. (2008) Fenites associated with carbonatites. Canadian Mineralogist, 46, 915-932.
1028 Lester, G.W., Clark, A.H., Kyser, T.K., and Naslund, H.R. (2013) Experiments on liquid
1029 immiscibility in silicate melts with H_2O, P, S, F and Cl: Implications for natural magmas.
1030 Contributions to Mineralogy and Petrology, 166, 329–349.
1031 Levin, E.M., Robbins, C., and Reser, M.K. (1964) Phase Diagrams for Ceramists. The Amnerican
1032 Ceramics Society.
1033 London, D. (1986) The magmatic-hydrothermal transition in the Tanco rare-element pegmatite:
1034 Evidence from fluid inclusions and phase equilibrium experiments. American Mineralogist,
1035 71, 376-395.
1036 London, D. (2008) Pegmatites. Mineralogical Association of Canada.
1037 Maas, R., Kinny, P.D., Williams, I.S., Froude, D.O., and Compston, W. (1992) The Earth's oldest
1038 known crust: A geochronological and geochemical study of 3900–4200 Ma old detrital

zircons from Mt. Narryer and Jack Hills Western Australia. Geochimica et Cosmochimica Acta, 56, 1281–1300.

Macdonald, R., Bagiński, B., Belkin, H.E., and Stachowicz, M. (2019) Composition, paragenesis, and alteration of the chevkinite group of minerals. American Mineralogist, 104, 348-369

Magnus, P.D. (2012) Scientific Enquiry and Natural Kinds: From Mallards to Planets. Palgrave MacMillan.

Maier, W.D. (2005) Platinum-group element (PGE) deposits and occurrences: Mineralization styles, genetic concepts, and exploration criteria. Journal of African Earth Science, 41, 165–191.

Maimon, O., and Rokarch, L. (2006) Clustering methods. In: Data Mining and Knowledge Discovery Handbook. Springer, pp. 321-352.

Marks, M.A.W., and Markl, G. (2017) A global review on agpaitic rocks. Earth Science Reviews, 173, 229-258.

Merlino, S., and Perchiazzi, N. (1988) Modular mineralogy in the cuspidine group of minerals. Canadian Mineralogist, 26, 933-943.

Mills, S.J., Hatert, F., Nickel, E.H., and Ferrais, G. (2009) The standardization of mineral group hierarchies: Application to recent nomenclature proposals. European Journal of Mineralogy, 21, 1073-1080.

Mitchell, R.H. [Ed.] (1996a) Undersaturated Alkaline Rocks: Mineralogy, Petrogenesis, and Economic Potential. Mineralogical Association of Canada, Short Course 24.

Mitchell, R.H. (1996b) Classification of undersaturated and related alkaline rocks. Mineralogical Association of Canada Short Course, 24, 1-22.

Mitchell, R.N., Spencer, C.J., Kirscher, U., and Wilde, S.A. (2022) Plate tectonic-like cycles since the Hadean: Initiated or inherited? Geology, 50, 827-831.

Morrison, S.M., and Hazen, R.M. (2020) An evolutionary system of mineralogy, part II: interstellar and solar nebula primary condensation mineralogy (> 4.565 Ga). American Mineralogist, 195, 1508-1535.

Morrison, S.M., and Hazen, R.M. (2021) An evolutionary system of mineralogy, part IV: Planetesimal differentiation and impact mineralization (4.566 to 4.560 Ga). American Mineralogist, 106, 730-761.

Morrison, S.M., Liu, C., Eleish, A., Prabhu, A., Li, C., Ralph, J., Downs, R.T., Golden, J.J., Fox, P., Hummer, D.R., Meyer, M.B., and Hazen, R.M. (2017) Network analysis of mineralogical systems. American Mineralogist, 102, 1588-1596.

Morrison, S.M., Buongiorno, J., Downs, R.T., Eleish, A., Fox, P., Giovannelli, D., Golden, J.J., Hummer, D.R., Hystad, G., Kellogg, L.H., Kreylos, O., Krivovichev, S.V., Liu, C., Prabhu, A., Ralph, J., Runyon, S.E., Zahirovic, S., and Hazen, R.M. (2020) Exploring carbon mineral systems: Recent advances in C mineral evolution, mineral ecology, and network analysis. Frontiers in Earth Sciences. DOI: 10.3389/feart.2020.00208

Morrison, S.M., Hazen, R.M., and Prabhu, A (2022) An evolutionary system of mineralogy, part VI: Earth's earliest Hadean crust (> 4370 Ma). American Mineralogist, 107, in press.

Moynier, F., Yin, Q.-Z., Boyet, M., Jacobsen, B., and Rosing, M.T. (2010) Coupled ^{182}W-^{142}Nd constraint for early Earth differentiation. Proceedings of the National Academy of Sciences USA, 107, 10810-10814.

Mungall, J.E., and Naldrett, A.J. (2008) Ore deposits of the platinum-group elements. Elements, 4, 253-258.

Nance, R.D., Murphy, J.B., and Santosh, M. (2014) The supercontinent cycle: A retrospective essay. Gondwana Research, 25, 4-29.

Newman, M.E.J. (2010) Networks: An Introduction. Oxford University Press.

O'Driscoll, B., and Van Tongeren, J.A. (2017) Layered intrusions: From petrological paradigms to precious metal repositories. Elements, 13, 383-389.

Ouzegane, K., Fourcade, S., Kienast, J.-R., and Javoy, M. (1988) New carbonatite complexes in the Archaean In'Ouzzal nucleus (Ahaggar, Algeria): Mineralogical and geochemical data. Contributions to Mineralogy and Petrology, 98, 277-292.

Philpotts, A.R., and Ague, J.J. (2009) Principles of Igneous and Metamorphic Petrology. Second Edition. Cambridge University Press.

Rastsvetaeva, R.K., and Chukanov, N.V. (2012) Classification of eudialyte-group minerals. Geology of Ore Deposits, 54, 487-497.

Rastsvetaeva, R.K., Chukanov, N.V., and Aksenov, S.M. (2016) The crystal chemistry of lamprophyllite-related minerals: a review. European Journal of Mineralogy, 28, 915-930.

Rollinson, H. (2007) Early Earth Systems: A Geochemical Approach. Blackwell Publishing.

Roycroft, P.D. (1991) Magmatically zoned muscovite from the peraluminous two-mica granites of the Leinster batholith, southeast Ireland. Geology, 19, 437-440.

Rudnick, R.L., and Gao, S. (2005) Composition of the continental crust. Treatise on Geochemistry, 3, 1–64.

Salvioli-Mariani, E., Boschetti, T., Toscani, L., Montanini, A., Petriglieri, J.R., and Bersani, D. (2020) Multi-stage rodingitization of ophiolite bodies from Northern Apennines (Italy): Constraints from petrography, geochemistry and thermodynamic modeling. Geoscience Frontiers, 1, 2103-2125.

Savelyev, D.P., Kamenetsky, V.S., Danyushevsky, L.V., Botcharnikov, R.E., Kamenetsky, M.B., Park, J.-W., Portnyagin, M.V., Olin, P., Krasheninnikov, S.P., and Hauff, F. (2018) Immiscible sulfide melts in primitive oceanic magmas: Evidence and implications from picrite lavas (Eastern Kamchatka, Russia). American Mineralogist, 103, 886–898.

Schertl, H.-P., Mills, S.J., and Maresch, W.V. (2018) A Compendium of IMA-Approved Mineral Nomenclature. International Mineralogical Association.

Shand, J.S. (1943) Eruptive Rocks: Their Genesis, Composition, Classification, with a Chapter on Meteorites, second edition. John Wiley and Sons.

Shrenk, M.O., Brazelton, W.J., and Lang, S.Q. (2013) Serpentinization, carbon, and deep life. Reviews in Mineralogy and Geochemistry, 75, 575-606.

Simandl, G.J., and Paradis, S. (2018) Carbonaites: Related ore deposits, resources, footprint, and exploration methods. Applied Earth Sciences, 117, 123-152.

Sizova, E., Gerya, T., and Brown, M. (2014) Contrasting styles of Phanerozoic and Precambrian continental collision. Gondwana Research, 25, 522-545.

Sizova, E., Gerya, T., Brown, M., and Perchuk, L.L. (2010) Subduction styles in the Precambrian: insight from numerical experiments. Lithos, 116, 209-229.

Sjöqvist, A.S.L., Cornell, D.H., Andersen, T., Christensson, U.I., and Berg, J.T. (2017) Magmatic age of rare-earth element and zirconium mineralisation at the Norra Kärr alkaline complex,

1125 southern Sweden, determined by U-Pb and Lu-Hf isotope analyses of metasomatic zircon
1126 and eudialyte. Lithos, 294-295, 73-86.

1127 Sokolova, E., and Cámara, F. (2017) The seidozerite supergroup of TS-block minerals:
1128 nomenclature and classification, with change of the following names: rinkite to rinkite-(Ce),
1129 mosandrite to mosandrite-(Ce), hainite to hainite-(Y) and innelite-1T to innelite-1A.
1130 Mineralogical Magazine, 81, 1457-1487,

1131 Speer, J.A. (1984) Micas in igneous rocks. Reviews in Mineralogy, 13, 299-356.

1132 Tassara, S., Ague, J.J., and Valencia, V. (2021) The deep magmatic cumulate roots of the Acadian
1133 orogen, eastern North America. Geology, 49, 168-173.

1134 Tilley, C.E. (1921) Reviews: Die Eruptivgesteine des Kristianiagebietes. IV. Das Fengebiet in
1135 Telemerk, Norwegen. By W.C. Brøgger. Vid. Selsk. Skrifter I.M.N.Kl. No. 9, pp. 1-408. 1920.
1136 Geological Magazine, 58, 549-554.

1137 Tkachev, A.V. (2011) Evolution of metallogeny of granitic pegmatites associated with orogens
1138 throughout geological time. Geological Society of London, Special Publications, 350, 7-23.

1139 Treetstra, D.K., and Černý, P. (1995) First natural occurrences of end-member pollucite: A
1140 product of low-temperature reequilibrium. European Journal of Mineralogy, 7, 1137-1148.

1141 Trønnes, R.G., Baron, M.A., Eigenmann, K.R., Guren, M.G., Heyn, B.H., Løken, A., and Mohn, C.E.
1142 (2019) Core formation, mantle differentiation and core-mantle interaction within Earth and
1143 the terrestrial planets. Tectonophysics, 760, 165-198.

1144 Valley, J.W., Cavosie, A.J., Ushikubo, T., Reinhard, D.A., Lawrence, D.F., Larson, D.J., Clifton, P.H.,
1145 Kelly, T.F., Wilde, S.A., Moser, D.E., and Spicuzza, M.J. (2014) Hadean age for a post-magma-
1146 ocean zircon confirmed by atom-probe tomography. Nature Geoscience, 7, 219-223.

Van Kranendonk, M.J., Smithies, R.H., and Bennett, V.C. [Editors] (2007) Earth's Oldest Rocks. Developments in Precambrian Geology, 15. Elsevier.

Wan, B., Yang, X., Tian, X., Yuan, H., Kirscher, U., and Mitchell, R.N. (2020) Seismological evidence for the earliest global subduction network at 2 Ga. Science Advances, 6, eabc5491 (9 p.).

Weidendorfer, D., Schmidt, M.W., and Mattsson, H.B. (2016) Fractional crystallization of Si-undersaturated alkaline magmas leading to unmixing of carbonatites on Brava Island (Cape Verde) and a general model of carbonatite genesis in alkaline magma suites. Contributions to Mineralogy and Petrology, 171, 43.

Whalen, J.B. (1985) Geochemistry of an island-arc plutonic suite: the Uasilau-Yau Yau intrusive complex, New Britain, P.N.G. Journal of Petrology, 26, 603-632.

Wilde, S.A., Valley, J.W., Peck, W.H., and Graham, C M. (2001) Evidence from detrital zircons for the existence of continental crust and oceans on the Earth 4.4. Gyr ago. Nature, 409, 175-178.

Woolley, A.R. (1987) Alkaline Rocks and Carbonatites of the World. Part 1: North and South America. British Museum (Natural History).

Woolley, A.R. (2001) Alkaline Rocks and Carbonatites of the World. Part 3: Africa. Geological Society of London.

Woolley, A.R. (2019) Alkaline Rocks and Carbonatites of the World. Part 4: Antarctica, Asia and Europe (Excluding the former USSR), Australasia and Oceanic Islands. Geological Society of London.

1168 Woolley, A.R., and Kjarsgaard, B.A (2008) Paragenetic types of carbonatite as indicated by the
1169 diversity and relative abundances of associated silicate rocks: evidence from a global
1170 database. Canadian Mineralogist, 46, 741-752.
1171 Xiong, F., Xingzhen, X., Mugnaioli, E., Gemmi, M., Wirth, R., Grew, E.S., Robinson, P.T., and
1172 Yang, J. (2020) Two new minerals, badengzhuite, TiP, and zhiqinite, $TiSi_2$, from the Cr-11
1173 chromitite orebody, Luobusa ophiolite, Tibet, China: is this evidence for super-reduced
1174 mantle-derived fluids? European Journal of Mineralogy, 32, 557-574.
1175 Xiong, Q., Griffin, W.L., Huang, J.-X., Gain, S.E.M., Toledo, V., Pearson, N.J., and O'Reilly, S.Y.
1176 (2017) Super-reduced mineral assemblages on "ophiolitic" chromitites and peridotites: the
1177 view from Mount Carmel. European Journal of Mineralogy, 29, 557-570.
1178 Yaxley, G.M., and Brey, G.P. (2004) Phase relations of carbonate-bearing eclogite assemblages
1179 from 2.5 to 5.5 GPa: Implications for petrogenesis of carbonatites. Contributions to
1180 Mineralogy and Petrology, 146, 606-619.
1181 Yaxley, G.M., Kjarsgaard, B.A., and Jaques, A.L. (2021) Evolution of carbonatite magmas in the
1182 upper mantle and crust. Elements, 17, 315-320.
1183 Yoder, H.S. Jr (1976) Generation of Basaltic Magma. National Academy of Sciences Press.
1184 Yoder, H.S. Jr (1979) The Evolution of the Igneous Rocks: Fiftieth Anniversary Perspectives.
1185 Princeton University Press.
1186 Yoder, H.S. Jr. (1992) Norman L. Bowen (1886-1956): MIT class of 1912. First predoctoral fellow
1187 of the Geophysical Laboratory. Earth Sciences History, 11, 45-55.
1188 Yoder, H.S. Jr. (1998) Norman L. Bowen: The experimental approach to petrology. GSA Today,
1189 May 1998, 10-11.

1190 Zaitsev, A.N., and Keller, J. (2006) Mineralogical and chemical transformation of Oldoinyo
1191 Lengai natrocarbonates, Tanzania. Lithos, 91, 191-207.
1192 Zaitsev, A.N., Wenzel, T., Vennemann, T, and Markl, G. (2013) Tindewret volcano, Kenya: an
1193 altered natrocarbonatite locality? Mineralogical magazine, 77, 213-226.
1194

Table 1. Catalog of 6 Supplementary Tables (see also associated Supplementary Read-Me Files) and 3 Interactive Graphical Figures (see figure captions for links and instructions).

Supplementary Table 1. A list of 1665 IMA-approved species that occur as primary igneous minerals, with compositions and distributions among 8 igneous rock types.

Supplementary Table 2. A list of 919 mineral kinds that occur as primary igneous phases, with compositions and distributions among 8 igneous rock types.

Supplementary Table 3. A matrix listing the modes of 1850 igneous rocks. We record the distribution of 115 of the most common primary igneous minerals among these rocks.

Supplementary Table 4. A 115 x 115 symmetrical matrix that records the frequencies of co-occurrence of mineral pairs in Table 3.

Supplementary Table 5. A 115 x 115 symmetrical matrix (derived from Table 5) that records the percentage of the less common mineral that co-occurs with the more common mineral.

Supplementary Table 6. A list matching 1001 IMA-approved species with their associated 251 mineral kinds, which are defined by lumping two or more species.

Interactive Figure 1. A unipartite network of coexistence among 115 of the most common primary igneous minerals, based on data in Supplementary Tables 3 and 5. The nodes are colored by communities, based on Louvain Community Detection.

Interactive Figure 2. A heatmap illustrating coexistence among 115 of the most common primary igneous minerals, based on data in Supplementary Tables 3 and 5. Minerals are arranged by Agglomerative Hierarchical Clustering.

Interactive Figure 5. A unipartite network of coexistence among 115 of the most common primary igneous minerals, based on data in Supplementary Tables 3 and 5. The nodes are colored by communities, based on Louvain Community Detection.

Table 2. Frequently occurring primary igneous minerals, with their abundances, common synonyms from the petrographic literature, and numbers of IMA species included in each mineral kind

Mineral Kind	Chemical Formula	Abundance[1]	Synonyms[2]	Community-Cluster[3]	#IMA[4]
Native Elements					
Graphite	C	5	plumbago	2-C-3	1
Sulfides					
Pyrite	FeS_2	288		4-D-4	1
Pyrrhotite	Fe_7S_8	64	pyrrhotine	2-B	1
Chalcopyrite	$CuFeS_2$	38		4-D-4	1
Galena	PbS	37		4-D-4	1
Molybdenite	MoS_2	11		4-D-4	1
Sphalerite	ZnS	30		4-D-4	1
Oxides					
Rutile	TiO_2	100	sagenite	4-D-1	1
Anatase	TiO_2	20		4-D-1	1
Brookite	TiO_2	6		4-B-2	1
Baddeleyite	ZrO_2	37		4-B-2	1
Cassiterite	SnO_2	21		1-A-1	1
Corundum	Al_2O_3	20		2-C-3	1
Uraninite	UO_2	9		1-A-1	1
Magnetite	$Fe^{2+}Fe^{3+}{}_2O_4$	1161	iron ore; martite	2-F	1
Chromite	$(Fe^{2+},Mg)Cr^{3+}{}_2O_4$	41		2-B-2	3

Hercynite	$Fe^{2+}Al_2O_4$	8	picotite	2-B-2	1
Spinel	$(Mg,Fe^{2+})(Al,Fe^{3+},Cr^{3+})_2O_4$	53	pleonaste	2-B-2	1
Ilmenite	$Fe^{2+}Ti^{4+}O_3$	330		2-B	1
Perovskite	$CaTi^{4+}O_3$	137	dysanalyte; knopite; loparite	2-B-2	1
Columbite	$(Fe,Mg)(Ta,Nb)_2O_6$	62		1-A-1	7
Euxenite	$(Y,Ca,Ce,U,Th)(Nb,Ta,Ti)_2O_6$	8		1-D-4	7
Fergusonite	$(Y,REE)(Nb,Ta)O_4$	7		4-D-4	7
Zirconolite	$(Ca,Y)Zr(Ti,Mg,Al)_2O_7$	9		4-B-2	4
Aeschynite	$(Y,REE,Ca,Th)(Ti,Nb,Ta)_2(O,OH)_6$	10		4-D-4	8
Pyrochlore	$(Na,Ca,Pb,Mn)_2Nb_2O_6(O,F,OH)$	172	betafite; hatchettolite; ralstonite	4-D-4	9
Microlite	$(Na,Ca,Pb,Mn)_2Ta_2O_6(O,F,OH)$	27		1-A-1	11
Halides					
Fluorite	CaF_2	213		3-D	1
Carbonates					
Calcite	$CaCO_3$	347	sovite/alvikite = calcite carbonatite	4-D	1
Dolomite	$CaMg(CO_3)_2$	99	beforsite/rauhaugite = dolomite carbonatite	4-D-4	1
Ankerite	$CaFe^{2+}(CO_3)_2$	50	ferrocarbonatite = ankerite/siderite carbonatite	4-D-4	1
Siderite	$FeCO_3$	11		4-D-4	1
Magnesite	$MgCO_3$	3		4-D-4	1
Strontianite	$SrCO_3$	26		4-D-4	1
Gregoryite	$Na_2(CO_3)$	2		5-E	1
Nyererite	$Na_2Ca(CO_3)_2$	3		5-E	1
Burbankite	$(Na,Ca)_3(Sr,Ba,Ce)_3(CO_3)_5$	7		4-D-4	3

Ancylite	$(La,Ce)Sr(CO_3)_2(OH)\cdot H_2O$	17		4-D-4	2
Bastnaesite	$(Y,REE)CO_3(F,OH)$	45		4-D-4	7
Parisite	$Ca(REE)_2(CO_3)_3F_2$	22		4-D-4	2
Synchesite	$(Ca,Ba)(Y,REE)(CO_3)_2F$	20		4-D-4	4
Sulphates					
Baryte	$BaSO_4$	79		4-D-4	1
Phosphates					
Fluorapatite	$Ca_5(PO_4)_3(F,OH,Cl)$	1234	dahllite; francolite; phoscorite = apatite-rich rock	4-F	1
Monazite	$(REE)PO_4$	94	cheralite; wiikite	4-D-4	4
Xenotime	$(Y,REE)(P,As)O_4$	23		1-D-1	3
Amblygonite	Li(Al,Fe3+)PO4(F,OH)	16		1-A-1	3
Nesosilicates or Orthosilicates					
Forsterite	Mg_2SiO_4	412	hortonolite; iddingsite; peridot	2-B	1
Fayalite	$Fe^{2+}{}_2SIO_4$	30		3-C-3	1
Monticellite`	$CaMgSiO_4$	24		2-B-2	1
Andradite	$Ca_3Fe3^{+}{}_2Si_3O_{12}$	199	melanite; schorlomite	2-C-3	3
Almandine	$Fe^{2+}{}_3Al_2Si_3O_{12}$	7		1-A-1	1
Spessartine	$Mn^{2+}{}_3Al_2Si_3O_{12}$	7		1-A-1	2
Clinohumite	$Mg_9(SiO_4)_4(F,OH)_2$	6		2-B-2	1
Zircon	$ZrSiO_4$	400		1-D	1
Thorite	$ThSiO_4$	30		1-D-4	1
Titanite	$CaTi^{4+}SiO_5$	518	sphene	2-D	2
Topaz	$Al_2SiO_4F_2$	26		1-A-1	1

Phenakite	Be_2SiO_4	9		1-A-1	1
Eucryptite	$LiAlSiO_4$	5		1-A-1	1
Britholite	$(Y,REE,Ca)_5(SiO_4)_3(OH,F)$	14	beckelite	3-C-4	5
Sorosilicates or Disilicates					
Mellilite	$(Ca,Na)_2(Mg,Fe^{2+},Al,Si)_3O_7$	83		2-B-2	3
Bertrandite	$Be_4Si_2O_7(OH)_2$	6		1-A-1	1
Allanite	$Ca(REE)Al_2Fe^{2+}(Si_2O_7)(SiO_4)O(OH)$	95	orthite; wiikite	2-C-4	9
Chevkinite	$(REE)_4(Ti^{4+},Fe^{2+},Fe^{3+},Zr,Mn,Cr,W,\ )_5O_8(Si_2O_7)_2$	14		3-C-4	6
Lamprophyllite	$(Sr,Ba)(Na,K)Ti^{4+}{}_2Na_3Ti^{4+}(Si_2O_7)_2O_2(OH)_2$	13		3-C-3	9
Rinkite	$(Na,Ca,Mn,Y,REE)_4(H_2O,\ )_2(Ti^{4+},Zr,Nb)(Si_2O_7)_2(OH,F)_{4-x}(H_2O)_x$	38		3-C-3	12
Wohlerite	$[(Na,Ca)(Ca,Mn^{2+},Fe^{2+})_2(Ti^{4+},Nb^{5+},Zr^{4+})(Si_2O_7)(O,F)_2$	35		3-C-3	5
Cyclosilicates					
Beryl	$(Na,Cs,\ )Be_2(Be,Li,B)(Al,Mg,Fe^{3+})_2Si_6O_{18}$	41	aquamarine; emerald; morganite	1-A-1	6
Tourmaline	$(\ ,Na,Ca)(Mg,Fe,Al)_3(Mg,Al)_6(Si_6O_{18})(BO_3)_3(OH,F)_3(OH,O)$	54		1-A-1	21
Elbaite	$Na(Al_{1.5}Li_{1.5})Al_6(Si_6O_{18})(BO_3)_3(OH)_3OH$	24		1-A-1	5
Catapleiite	$(Na2,Ca)Zr(Si_3O_9)\cdot 2H_2O$	13		3-C-3	2
Eudialyte	$Na_{15}Ca_6Fe^{2+}{}_3Zr^{4+}{}_3Si(Si_{25}O_{73})(O,OH,H_2O)_3(Cl,OH)_2$	69	eucolite	3-C-3	30
Inosilicates					
Aegirine	$(Ca,Na)(Fe^{3+},Mg,Fe^{2+})Si_2O_6$	521	acmite	3-D	2
Augite	$(Ca,Mg,Fe^{2+},Fe^{3+})_2(Si,Al)_2O_6$ [0.15 < $CaSiO_3$ < 0.45]	504		2-B	1
Pigeonite	$(Mg,Fe^{2+},Ca)SiO_3$ [0.05 < $CaSiO_3$ < 0.15]	16		2-B-2	1
Diopside	$CaMgSi_2O_6$	228	diallage; fassaite; malacolite; salite; uralite	2-B	1
Hedenbergite	$CaFe^{2+}Si_2O_6$	15		2-C-3	1

Spodumene	$LiAlSi_2O_6$	24			1-A-1	1
Orthoenstatite	$(Mg,Fe^{2+})SiO_3$	135	bronzite; hypersthene		2-B-2	1
Wollastonite	$CaSiO_3$	15			3-C-3	1
Hornblende	$(Na,K)Ca_2(Mg,Fe^{2+},Al,Fe^{3+})_5(Si,Al)_8O_{22}(OH,F,Cl)_2$	487	barkevikite		2-B	18
Kaersutite	$NaCa_2[Mg_3(Al,Fe^{3+})Ti^{4+}](Si_6Al_2)O_{22}O_2$	19			2-B-3	2
Richterite	$Na(CaNa)(Mg,Fe^{2+})_5(Si,Al,Fe^{3+})_8O_{22}(OH)_2$	47			2-C-2	12
Arfvedsonite	$NaNa_2(Fe^{2+}{}_4Fe_{3+})Si_8O_{22}(OH)_2$	229			3-C	10
Riebeckite	$Na_2[(Fe^{2+},Mg)_3Fe^{3+}{}_2]Si_8O_{22}(OH,F)_2$	68	crocidolite; osannite		3-C-3	3
Actinolite	$Ca_2(Mg,Fe^{2+})_5Si_8O_{22}(OH,F)_2$	10			4-B-2	1
Pectolite	$(Na,Li)(Ca,Mn^{2+})_2Si_3O_8(OH)$	12			3-C-3	3
Astrophyllite	$(K,Na,Li,Cs,\ ,Ca)_3(Fe^{2+},Mn^{2+},Mg,Na)_7(Ti^{4+},Zr,Nb)_2(Si_4O_{12})_2O_2(OH)_4(OH,O,F)(H_2O)_n$	37			3-C-3	12
Aenigmatite	$Na_4[Fe^{2+}{}_{10}Ti_2]O_4[Si_{12}O_{36}$	53			3-C-3	1
Phyllosilicates						
Biotite	$KFe^{2+}{}_2(Fe^{2+},Mg,Mn^{2+})(Si,Al,Fe^{3+})_2Si_2O_{10}(OH,F,Cl)_2$	888	anomite		2-D	6
Phlogopite	$[[KMg_2(Mg,Fe^{2+},Mn^{2+},Fe^{3+},Ti^{4+})(Si,Al,Fe^{3+})_2Si_2O_{10}(OH,F)_2]]$	176			4-B-2	6
Muscovite	$(K,Cs)(Al,V,Fe^{3+},Cr)_2(Si_3Al)O_{10}(OH)_2$	127			1-A-1	4
Lepidolite	$(K,Cs,Rb)(\ ,Li,Mg,Mn,Fe,Al,Ti)_3(Al,Si)_4O_{10}(F,OH,O)_2$	42			1-A-1	11
Petalite	$LiAlSi_4O_{10}$	19			1-A-1	1
Tectosilicat						
Quartz	SiO_2	531			1-A	1
Tridymite	SiO_2	5			2-C-3	1
Obsidian	(~90 wt % SiO_2 + Al_2O_3)	5			3-C-3	0
Albite	$NaAlSi_3O_8$	543	sodaclase; anorthoclase;			

				soda-orthoclase; oligoclase	1-A	1
	Anorthite	$CaAl_2Si_2O_8$	245	calciclase; bytownite	2-B	1
	Plagioclase	$(Na,Ca)Al(Al,Si)_3O_8$	210	andesine; labradorite	2-B	0
	Perthite	$(Na,K)AlSi_3O_8$	304		3-C	0
	Sanidine	$KAlSi_3O_8$	82		3-C-3	1
	Microcline	$KAlSi_3O_8$	310		1-A	1
	Orthoclase	$KAlSi_3O_8$	447		2-B	1
	Nepheline	$Na_3K(Al_4Si_4O_{16})$	567	eleoite; liebenerite; pinite; urtite	3-D	2
	Sodalite	$Na_4Si_3Al_3O_{12}Cl$	158		3-C-3	1
	Hauyne	$Na_3Ca(Si_3Al_3)O_{12}[(S^{6+}O_4),(H_2O)]$	63	hauynite; noselite	3-C-3	3
	Kalsilite	$(K,Na)AlSiO_4$	6		2-B-2	5
	Leucite	$KAlSi_2O_6$	103		2-B-3	1
	Cancrinite	$(Na,Ca,\ )_8(Al_6Si_6)O_{24}(CO_3,SO_4)_2{\cdot}2H_2O$	119		3-C-3	23
	Scapolite	$(Na,Ca)_4(Al,Si)_{12}O_{24}(CO_3,SO_4,Cl)$	12		2-C-3	3
	Analcime	$NaAlSi_2O_6{\cdot}H_2O$	146	analcite	2-C-3	1
	Natrolite	$(Na,Ca)_2(Si_3Al_2)O_{10}{\cdot}2H_2O$	17		3-C-3	1
	Pollucite	$Cs(Si_2Al)O_6{\cdot}nH_2O$	22		1-A-1	1
	Silicate Glass	(Si,Al,Ca,Mg,Fe,O; SiO_2 < 70 wt %)	48		2-B-3	0

[1] Number of occurrences in a survey of the modes of 1850 igneous rocks; see Supplementary Table 4.

[2] Includes names for alteration products (e.g., “pseudoleucite” is a mixture of phases derived from primary *leucite*) and intermediate compositions (e.g., “hortonolite” is Fe-bearing *forsterite*).

[3] The first number (1 to 5) refers to the community number in Figure 1A. The letters (A to F) refer to heatmap clusters in Figures 2 and 3A to 3D. The second number (1 to 4), when present, refers to the community number in Figure 5.

[4] The number of IMA-approved mineral species lumped into this mineral kind (see Supplementary Table 3). For example, *tourmaline* (which is not an IMA-approved mineral name) includes 20 IMA species. Note that *obsidian*, *perthite*, *plagioclase*, and *silicate glass* are not IMA-approved names and do not correspond to any IMA species.

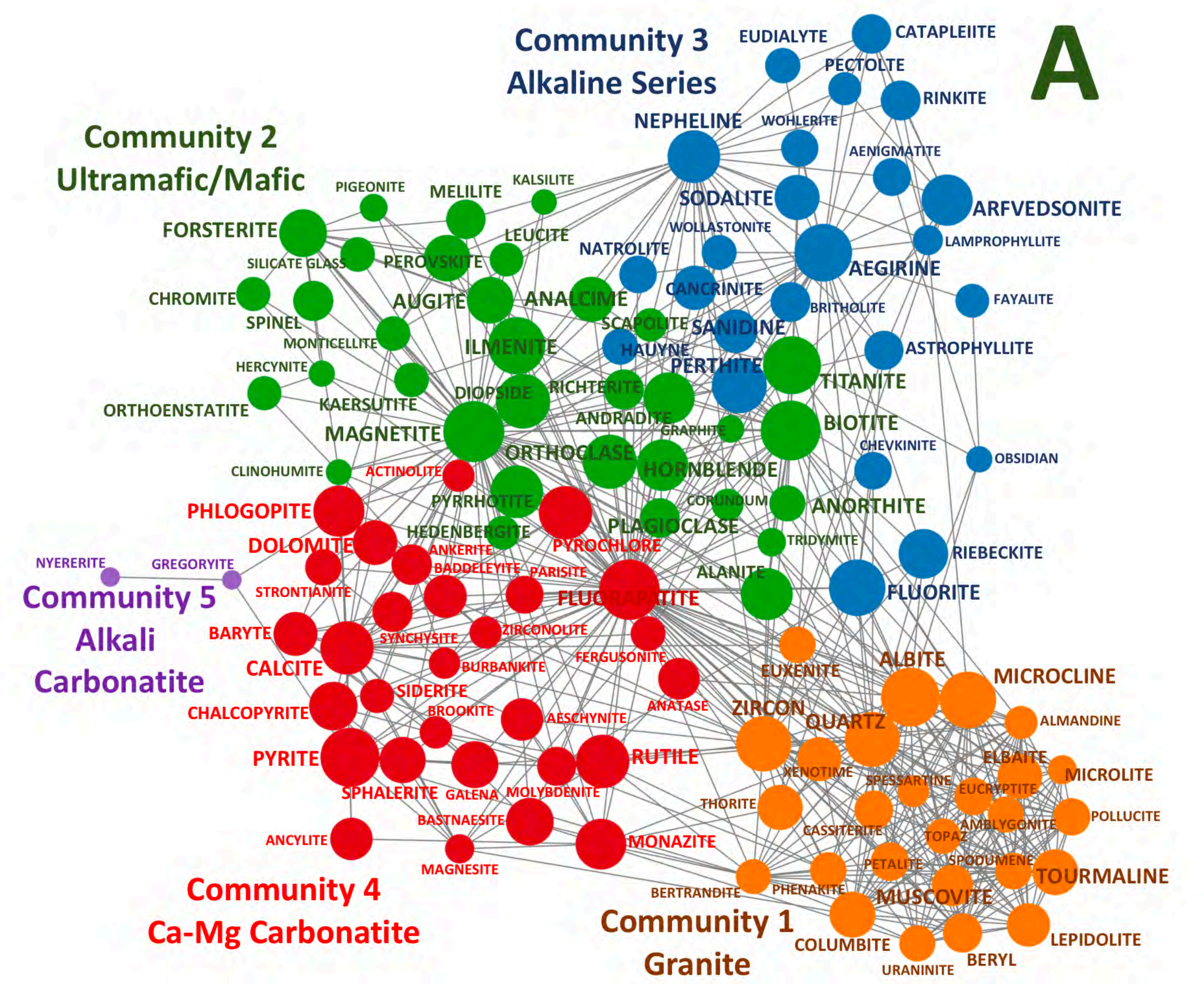
A
Community 3
Alkaline Series
EUDIALYTE
CATAPLEIITE
PECTOLTE
RINKITE
NEPHELINE
WOHLERITE
AENIGMATITE
Community 2
Ultramafic/Mafic
PIGEONITE
MELILITE
KALSILITE
SODALITE
ARFVEDSONITE
FORSTERITE
WOLLASTONITE
LEUCITE
LAMPROPHYLLITE
NATROLITE
SILICATE GLASS
PEROVSKITE
AEGIRINE
CHROMITE
AUGITE
ANALCIME
CANCRINITE
FAYALITE
BRITHOLITE
SPINEL
SCAPOLITE
SANIDINE
MONTICELLITE
ILMENITE
HAUYNE
ASTROPHYLLITE
PERTHITE
HERCYNITE
TITANITE
RICHTERITE
DIOPSIDE
ORTHOENSTATITE
KAERSUTITE
ANDRADITE
BIOTITE
MAGNETITE
GRAPHITE
CHEVKINITE
ORTHOCLASE
OBSIDIAN
CLINOHUMITE
ACTINOLITE
HORNBLENDE
PYRRHOTITE
CORUNDUM
ANORTHITE
PHLOGOPITE
HEDENBERGITE
PLAGIOCLASE
TRIDYMITE
RIEBECKITE
DOLOMITE
ANKERITE
PYROCHLORE
NYERERITE
GREGORYITE
BADDELEYITE
PARISITE
ALANITE
FLUORITE
STRONTIANITE
FLUORAPATITE
Community 5
Alkali
Carbonatite
BARYTE
SYNCHYSITE
ZIRCONOLITE
FERGUSONITE
EUXENITE
ALBITE
MICROCLINE
CALCITE
BURBANKITE
SIDERITE
ZIRCON
QUARTZ
ALMANDINE
CHALCOPYRITE
BROOKITE
AESCHYNITE
ANATASE
ELBAITE
XENOTIME
SPESSARTINE
MICROLITE
PYRITE
RUTILE
EUCRYPTITE
THORITE
POLLUCITE
SPHALERITE
GALENA
MOLYBDENITE
CASSITERITE
AMBLYGONITE
TOPAZ
BASTNAESITE
ANCYLITE
MONAZITE
PETALITE
SPODUMENE
TOURMALINE
MAGNESITE
BERTRANDITE
PHENAKITE
MUSCOVITE
Community 4
Ca-Mg Carbonatite
Community 1
Granite
COLUMBITE
LEPIDOLITE
BERYL
URANINITE

B

Olivine
Gabbro

Nepheline
Syenite

Calcite
Carbonatite

Muscovite
Granite

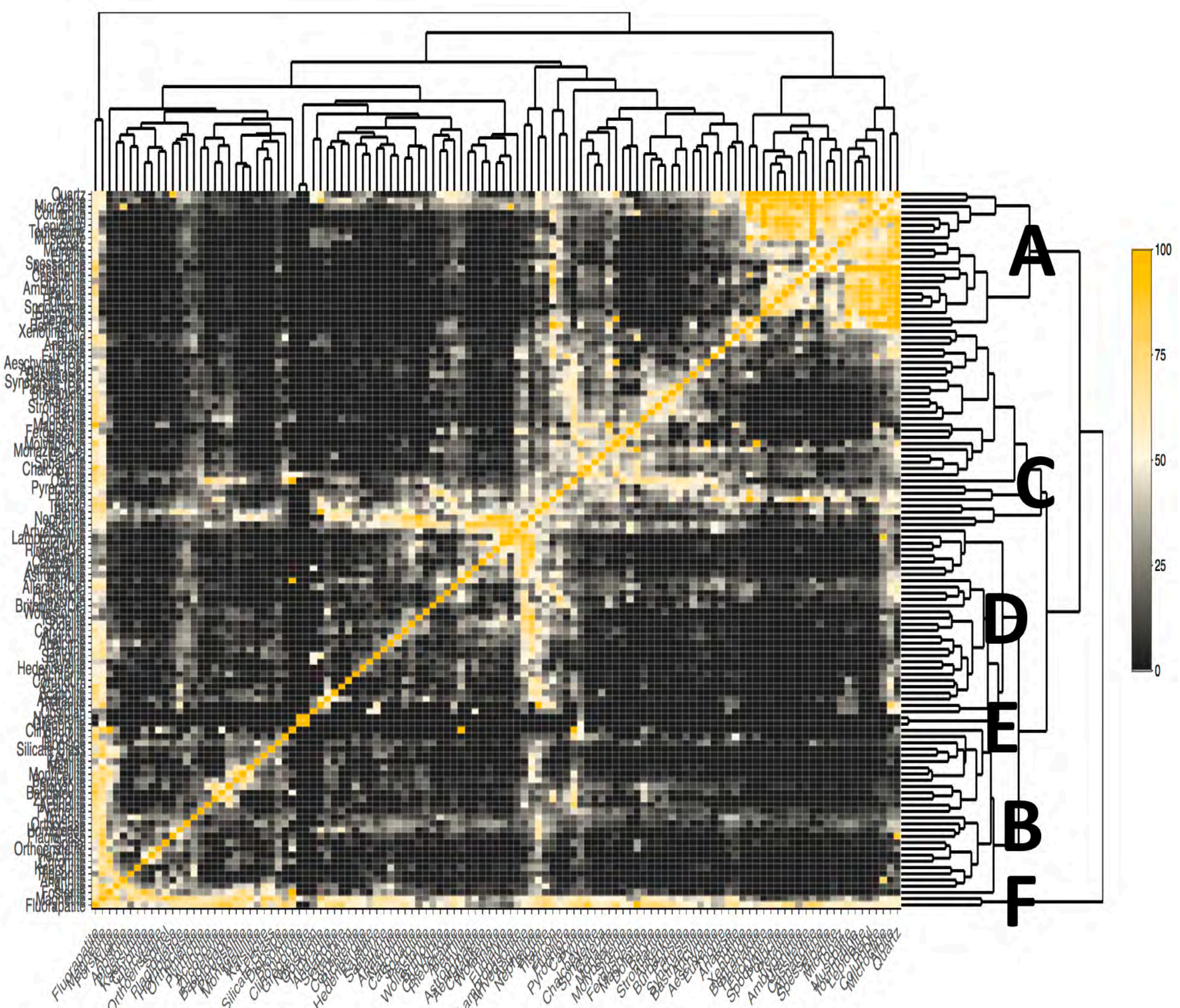
A
C
D
E
B
F
100
75
50
25
0

A

GRANITIC ROCKS

Bertrandite
Phenakite
Eucryptite
Spodumene
Pollucite
Petalite
Amblygonite
Uraninite
Cassiterite
Almandine
Spessartine
Elbaite
Microlite
Topaz
Muscovite
Tourmaline
Lepidolite
Beryl
Columbite
Microcline
Albite
Quartz

B

MAFIC/ULTRAMAFIC ROCKS

Fluorapatite
Magnetite
Forsterite
Augite
Anorthite
Pigeonite
Kaersutite
Chromite
Hercynite
Orthoenstatite
Spinel
Plagioclase
Hornblende
Orthoclase
Ilmenite
Pyrrhotite
Actinolite
Zirconolite
Baddeleyite
Phlogopite
Pervoskite
Monticellite
Melilite
Kalsilite
Leucite
Silicate.Glass
Diopside
Brookite
Clinohumite

ALKALINE IGNEOUS ROCKS

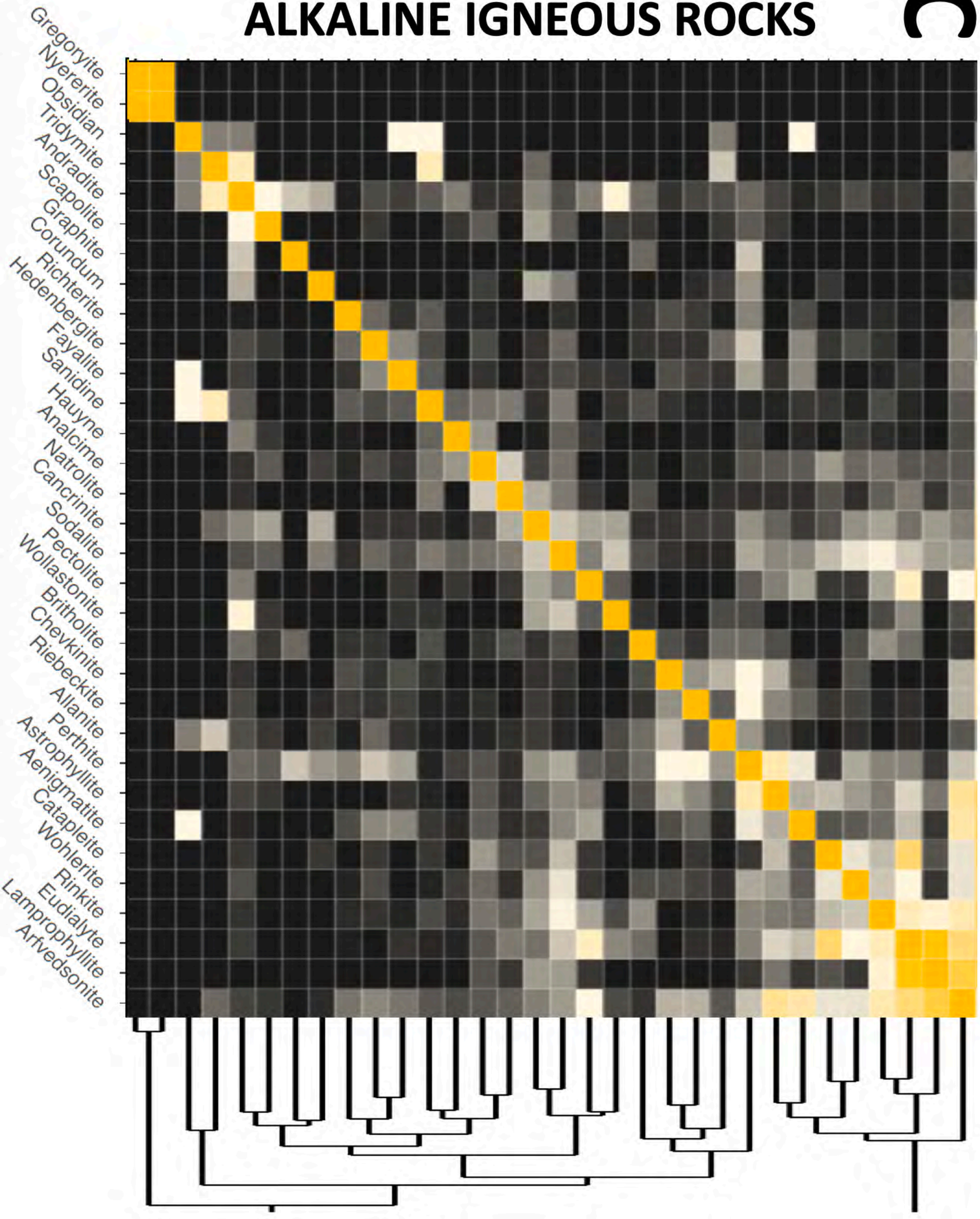

D

CARBONATITES

Aegirine
Nepheline
Biotite
Titanite
Zircon
Fluorite
Pyrochlore
Calcite
Pyrite
Chalcopyrite
Sphalerite
Galena
Monazite
Molybdenite
Siderite
Fergusonite
Magnesite
Dolomite
Baryte
Strontianite
Ankerite
Burbankite
Parisite
Synchysite
Bastnaesite
Ancylite
Aeschynite
Euxenite
Thorite
Anatase
Rutile
Xenotime

Lamprophyllite
Eudialyte
Rinkite-(Ce)
Wohlerite
Catapleiite
Aenigmatite
Astrophyllite
Perthite
Allanite-(Ce)
Riebeckite
Chevkinite
Britholite-(Ce)
Wollastonite
Pectolite
Sodalite
Cancrinite
Natrolite
Analcime
Hauyne
Sanidine
Fayalite
Hedenbergite
Richterite
Corundum
Graphite
Scapolite
Andradite
Tridymite
Obsidian
Nyerereite
Gregoryite
Clinohumite
Brookite
Diopside
Silicate Glass
Leucite
Kalsilite
Melilite
Monticellite
Perovskite
Phlogopite
Baddeleyite
Zirconolite
Actinolite
Pyrrhotite
Ilmenite
Orthoclase
Hornblende
Plagioclase
Spinel
Orthoenstatite
Hercynite
Chromite
Kaersutite
Pigeonite
Anorthite
Augite
Fosterite

...copyrite
Sphalerite
Galena
Monazite
Molybdenite
Siderite
Fergusonite
Magnesite
Dolomite
Baryte
Strontianite
Ankerite
Burbankite
Parisite
Synchysite
Bastnaesite
Ancylite
Aeschynite
Euxenite
Thorite
Anatase
Rutile
Xenotime
Bertrandite
Phenakite
Eucryptite
Spodumene
Pollucite
Petalite
Amblygonite
Uraninite
Cassiterite
Almandine
Spessartine
Elbaite
Microlite
Topaz
Muscovite
Tourmaline
Lepidolite
Beryl
Columbite

MINERAL ANTIPATHIES

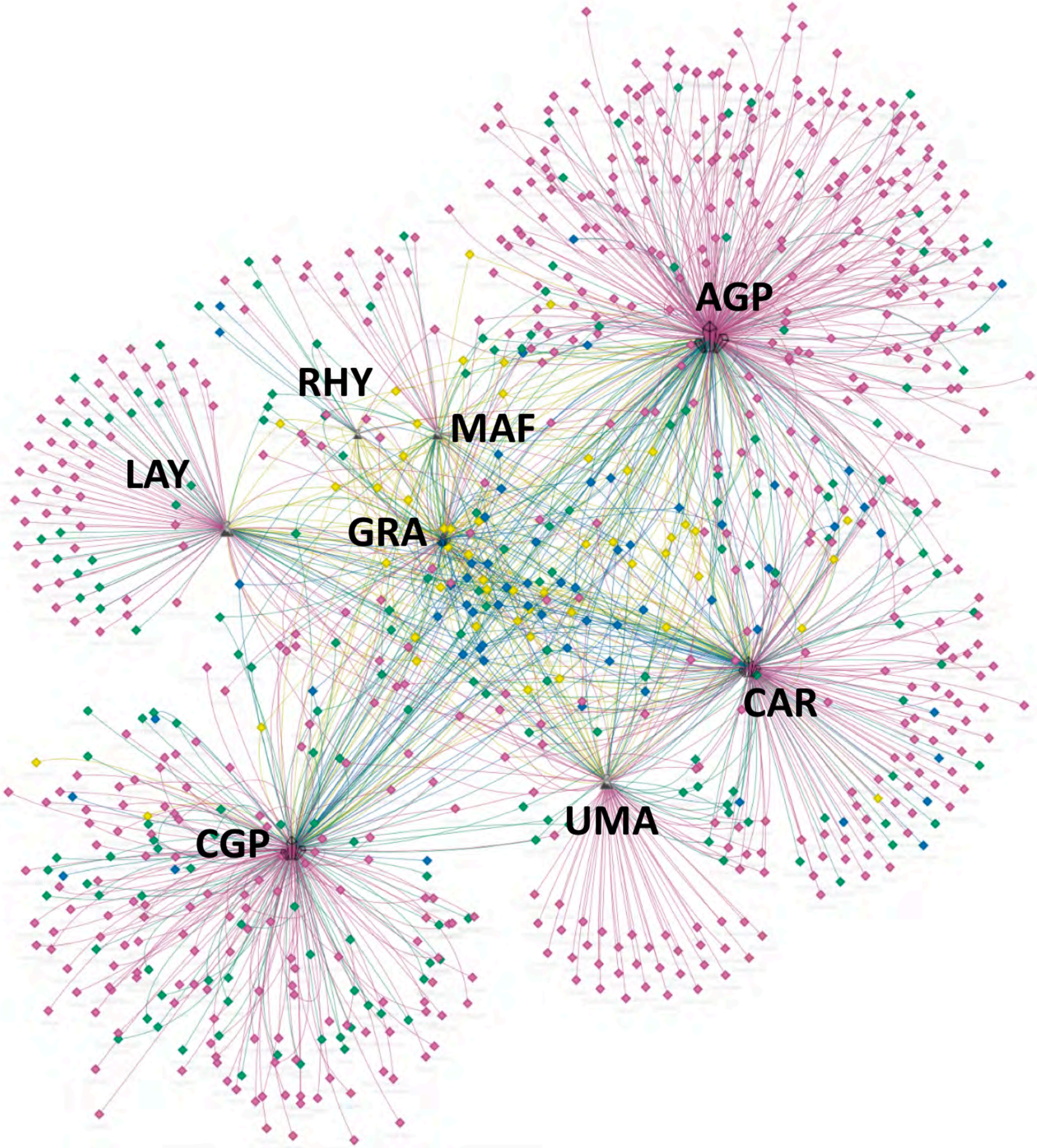
AGP
RHY
MAF
LAY
GRA
CAR
UMA
CGP

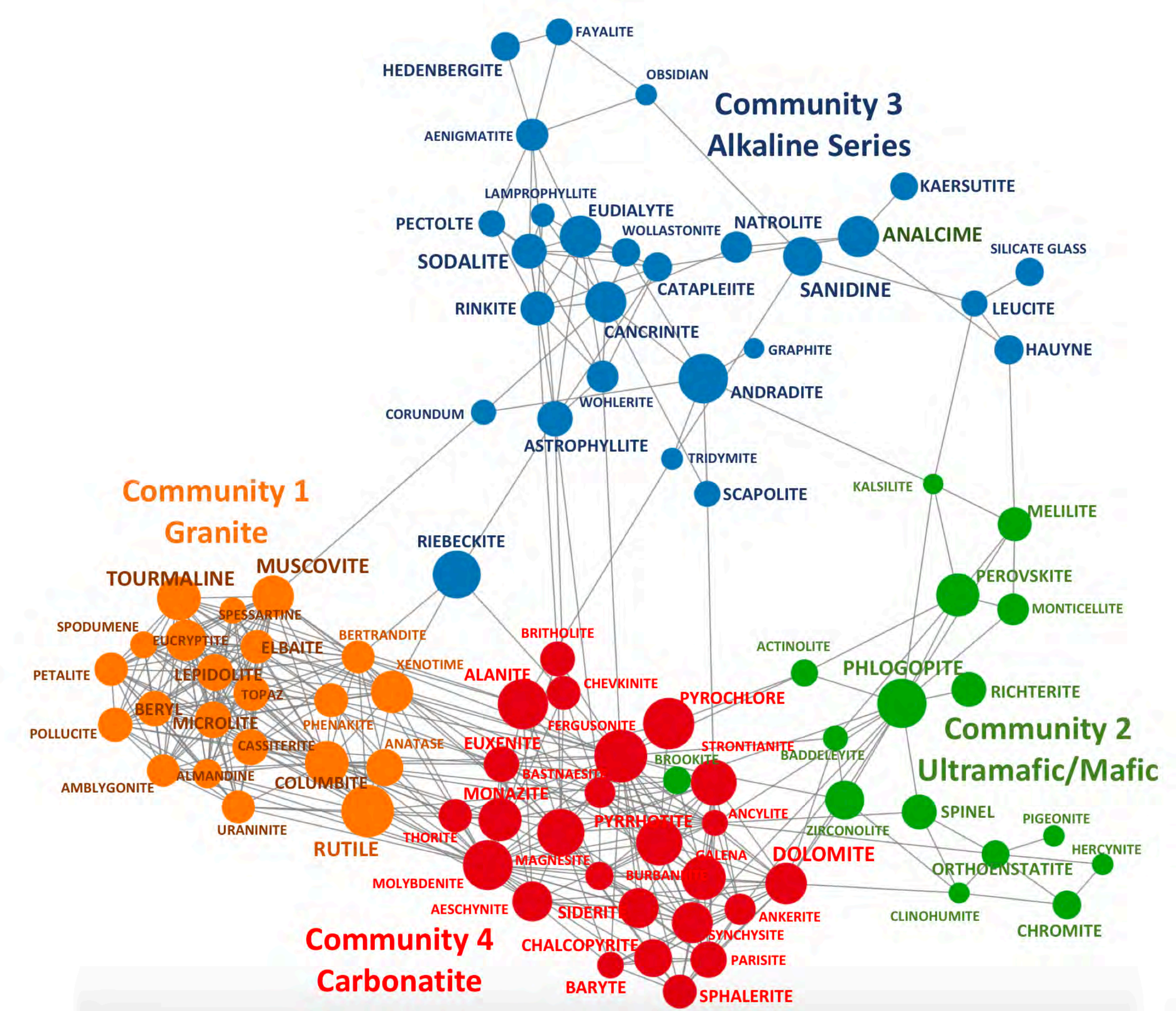
Community 3
Alkaline Series
Community 1
Granite
Community 2
Ultramafic/Mafic
Community 4
Carbonatite
FAYALITE
HEDENBERGITE
OBSIDIAN
AENIGMATITE
KAERSUTITE
LAMPROPHYLLITE
EUDIALYTE
PECTOLTE
WOLLASTONITE
NATROLITE
ANALCIME
SILICATE GLASS
SODALITE
CATAPLEIITE
SANIDINE
LEUCITE
RINKITE
CANCRINITE
GRAPHITE
HAUYNE
ANDRADITE
WOHLERITE
CORUNDUM
ASTROPHYLLITE
TRIDYMITE
SCAPOLITE
KALSILITE
MELILITE
RIEBECKITE
MUSCOVITE
TOURMALINE
PEROVSKITE
SPESSARTINE
MONTICELLITE
SPODUMENE
EUCRYPTITE
ELBAITE
BERTRANDITE
BRITHOLITE
ACTINOLITE
PETALITE
LEPIDOLITE
XENOTIME
ALANITE
CHEVKINITE
PHLOGOPITE
RICHTERITE
TOPAZ
PYROCHLORE
BERYL
MICROLITE
PHENAKITE
FERGUSONITE
POLLUCITE
CASSITERITE
ANATASE
EUXENITE
STRONTIANITE
BADDELEYITE
BROOKITE
AMBLYGONITE
ALMANDINE
COLUMBITE
BASTNAESITE
MONAZITE
SPINEL
PIGEONITE
ANCYLITE
PYRRHOTITE
ZIRCONOLITE
URANINITE
RUTILE
THORITE
DOLOMITE
HERCYNITE
MAGNESITE
GALENA
ORTHOENSTATITE
MOLYBDENITE
BURBANKITE
AESCHYNITE
SIDERITE
ANKERITE
CLINOHUMITE
CHROMITE
SYNCHYSITE
CHALCOPYRITE
PARISITE
BARYTE
SPHALERITE